

# Nearly Optimal Learning using Sparse Deep ReLU Networks in Regularized Empirical Risk Minimization with Lipschitz Loss

Ke Huang<sup>1</sup>, Mingming Liu<sup>1</sup>, Shujie Ma<sup>1</sup>

<sup>1</sup>Department of Statistics, University of California, Riverside, Riverside 92521, California, United States

**Keywords:** Classification, curse of dimensionality, deep neural networks, lipschitz loss function, ReLU, robust regression

## Abstract

We propose a sparse deep ReLU network (SDRN) estimator of the regression function obtained from regularized empirical risk minimization with a Lipschitz loss function. Our framework can be applied to a variety of regression and classification problems. We establish novel non-asymptotic excess risk bounds for our SDRN estimator when the regression function belongs to a Sobolev space with mixed derivatives. We obtain a new nearly optimal risk rate in the sense that the SDRN estimator can achieve nearly the same optimal minimax convergence rate as one-dimensional nonparametric regression with the dimension only involved in a logarithm term when the feature dimension is fixed. The estimator has a slightly slower rate when the dimension grows with the sample size. We show that the depth of the SDRN estimator grows with the sample size in logarithmic order, and the total number of nodes and weights grows in polynomial order of the sample size to have the nearly optimal risk rate. The proposed SDRN

can go deeper with fewer parameters to well estimate the regression and overcome the overfitting problem encountered by conventional feed-forward neural networks.

## **1 Introduction**

Advances in modern technologies have facilitated the collection of large-scale data that are growing in both sample size and the number of variables. Although conventional parametric models, such as generalized linear models are convenient for studying the relationships between variables, they may not be flexible enough to capture complex patterns in large-scale data. With a large sample size, the bias due to model misspecification becomes more prominent compared to sampling variability, and may lead to false conclusions. The problem of model misspecification can be solved by nonparametric regression methods that are capable of approximating the unknown target function well without a restrictive structural assumption. Theoretically, we hope that both the bias and the variance of the functional estimator decrease as the sample size increases. Moreover, the bias is reduced by increasing the variance and vice versa, so that a tradeoff between bias and variance can be achieved for an accurate prediction.

In the classical multivariate regression context with a smoothness condition imposed on the target function, the conventional nonparametric smoothing methods such as local kernels and splines (e.g. Stone, 1994; Cheng, Fan, & Marron, 1994; Fan & Gijbels, 1996; Ruppert, 1997; Wasserman, 2006; Ma, Racine, & Yang, 2015) suffer from the so-called “curse of dimensionality” (Bellman, 1961), i.e., the convergence rate of the resulting functional estimator deteriorates sharply as the dimension of the predictors increases. As such it is desirable to develop analytic tools that can alleviate the curse of dimensionality while preserving sufficient flexibility, to accommodate the large volume as well as the high dimensionality of the modern data.

In recent years, the investigation of statistical properties for regression using deep neural networks has received increasing attention in the statistical and machine learning communities. Deep neural networks with multiple hidden layers are powerful and ef-

fective machine learning tools for prediction and classification, and have been successfully applied to many fields, including computer vision, language processing, speech recognition, time series forecasting, and biomedical studies (e.g. Anthony & Bartlett, 2009; LeCun, Bengio, & Hinton, 2015; Schmidhuber, 2015; Liang & Srikant, 2017; Wang & Chen, 2018; Y. Chen, Segovia-Dominguez, & Gel, 2021; Fan, Ma, & Zhong, 2021). Several pioneering works (e.g. Bauer & Kohler, 2019; Schmidt-Hieber, 2020; M. Chen, Jiang, Liao, & Zhao, 2022) have established convergence rates for neural network estimators of a regression function when it has a compositional structure (e.g. Poggio, Mhaskar, Rosasco, Miranda, & Liao, 2017; Mhaskar, Liao, & Poggio, 2017; Bauer & Kohler, 2019; Schmidt-Hieber, 2020), or the covariates are assumed to lie in a low-dimensional manifold (e.g. Cheng & Wu, 2013; Shaham, Cloninger, & Coifman, 2018; Nakada & Imaizumi, 2020; Z. Shen, Yang, & Zhang, 2020; M. Chen et al., 2022). The compositional structure or the low-dimensional manifold assumption is assumed to alleviate the dimensionality problem. Moreover, most existing works (e.g. Kohler & Mehnert, 2011; Bauer & Kohler, 2019; Schmidt-Hieber, 2020; M. Chen et al., 2022; Lin, Wang, Wang, & Zhou, 2022) estimate the regression function using the least-squares method.

In this paper, we develop novel non-asymptotic excess risk bounds and convergence rates for a sparse deep ReLU network (SDRN) estimator of the regression function through regularized empirical risk minimization (ERM) with a Lipschitz loss function satisfying mild conditions.  $L_2$  regularization is employed by our approach to prevent possible over-fitting. We consider a unified framework in which the family of the loss functions is a general class. It includes the quadratic, Huber, quantile, and logistic loss functions as special cases, so many regression and classification problems can be solved by our framework. Classification (e.g. Kotsiantis, 2007; Kůrková & Sanguineti, 2019) is a crucial task of supervised learning, and robust regression is an important tool for analyzing data with heavy tails. We adopt a network structure of sparsely connected deep neural networks with the rectified linear unit (ReLU) activation function given in (Montanelli & Du, 2019) that allows the network to go deeper with fewer parame-

ters than the conventional feedforward neural networks (FNNs), so it enjoys parsimony, scalability, and lower computational complexity, which are important for deep learning models (Bengio & LeCun, 2007; Eldan & Shamir, 2016; Mhaskar & Poggio, 2016; Mhaskar et al., 2017). On the contrary, conventional FNNs can be computationally expensive and may suffer from overfitting (Srivastava, Hinton, Krizhevsky, Sutskever, & Salakhutdinov, 2014). Different from (Montanelli & Du, 2019) which focuses on finding a sparse neural network with known and given weights to approximate a target function, we obtain the SDRN estimator of a regression function with unknown weights trained through minimizing the regularized ERM. We also establish a new nearly optimal risk rate for the SDRN estimator when the regression function belongs to the Sobolev spaces of functions with square-integrable mixed second derivatives (also called Korobov spaces), commonly assumed for the sparse grid approaches dealing with high-dimensional partial differential equations (Bungartz & Griebel, 2004; Griebel, 2006; J. Shen & Wang, 2010; Montanelli & Du, 2019; Mao & Zhou, 2022a). This rate can break the notorious ‘curse of dimensionality’ suffered by the conventional nonparametric methods.

The main contributions of our paper are summarized as follows:

- We derive novel non-asymptotic excess risk bounds for the sparse deep ReLU network (SDRN) estimator obtained from regularized empirical risk minimization. The SDRN architecture allows the network to go deeper with fewer parameters than the regular FNNs, and it can overcome the overfitting problem suffered by conventional FNNs. Our established risk bounds consist of the estimation and approximation errors, for both of which we derive explicit forms as a function of the sample size, dimension of the feature space, and network complexity. The existing work (Montanelli & Du, 2019) uses an accuracy value  $\epsilon > 0$  for the approximation error only without data fitting. Moreover, we derive a new non-asymptotic bound for the network complexity. This bound has not been provided in (Montanelli & Du, 2019). These newly established bounds provide important theoretical guidance on how the network complexity should be related to the sample size and the dimension, so that a tradeoff between the

two errors can be achieved to secure an optimal fitting from the dataset.

- We show that the SDRN estimator can break the *curse of dimensionality* when the regression function is in the Korobov space by allowing the covariate dimension  $d$  to increase with sample size  $n$  with a rate slightly slower than  $\log(n)$ . The existing works on FNN regression, for example, (Bauer & Kohler, 2019) and (Schmidt-Hieber, 2019), still require the dimension  $d$  to be fixed. We further show that our SDRN estimator can achieve nearly the optimal minimax convergence rate as one-dimensional non-parametric regression with the dimension  $d$  only involved in a logarithm term when the dimension is fixed. The SDRN estimator has a suboptimal rate (slightly slower than the optimal rate) when the dimension increases with the sample size.
- We provide an architecture of the SDRN, and estimate the unknown parameters (unknown weights) in the SDRN through regularized ERM with Lipschitz loss, while (Montanelli & Du, 2019) focus on the study of the approximation of the sparse neural network with given and known weights to the target function. In addition, our SDRN can be applied to both regression and classification problems. We discuss several commonly used loss functions that satisfy the Lipschitz condition.
- We show that the depth of SDRN increases with the sample size  $n$  at a logarithmic rate, and the number of nodes and weights only need to grow with  $n$  at a polynomial rate to ensure the convergence properties of the SDRN estimator. The proposed SDRN can go deeper with fewer parameters to well estimate the regression and overcome the overfitting problem encountered by conventional FNNs.

The paper is organized as follows. Section 2 provides the basic setup, Section 3 discusses approximation of the target function by the ReLU networks, Section 4 constructs the sparse deep ReLU network (SDRN) estimator, Section 5 establishes the theoretical properties for the SDRN estimator obtained from empirical risk minimization, Section 6 further discusses the conditions imposed on the loss function, Section 7 reports results

from simulation studies, and Section 8 illustrates the proposed method through real data applications. Some concluding remarks are given in Section 9. All the technical proofs are provided in the Appendix.

**Notations:** Let  $\mathbf{a}_d = (a, \dots, a)^\top$  be a  $d$ -dimensional vector of  $a$ 's. let  $|A|$  be the cardinality of a set  $A$ . The vectorization of a  $m \times n$  matrix  $\mathbf{A}$ , denoted  $\text{vec}(\mathbf{A})$ , is the  $mn \times 1$  column vector by stacking the columns of the matrix  $\mathbf{A}$ . Denote  $\|\mathbf{a}\|_p = (\sum_{i=1}^m |a_i|^p)^{1/p}$  as the  $L^p$ -norm of a vector  $\mathbf{a} = (a_1, \dots, a_m)^\top$ , and  $\|\mathbf{a}\|_\infty = \max_{i=1, \dots, m} |a_i|$ . For two vectors  $\mathbf{a} = (a_1, \dots, a_m)^\top$  and  $\mathbf{b} = (b_1, \dots, b_m)^\top$ , denote  $\mathbf{a} \cdot \mathbf{b} = \sum_{i=1}^m a_i b_i$ . Moreover, for any arithmetic operations involving vectors, they are performed element-by-element. For any two values  $a$  and  $b$ , denote  $a \vee b = \max(a, b)$ . For two sequences of positive numbers  $a_n$  and  $b_n$ ,  $a_n \ll b_n$  means that  $b_n^{-1} a_n = o(1)$ ,  $a_n \lesssim b_n$  means that there exists a constant  $C \in (0, \infty)$  and  $n_0 \geq 1$  such that  $a_n \leq C b_n$  for  $n \geq n_0$ , and  $a_n \asymp b_n$  means that there exist constants  $C, C' \in (0, \infty)$  and  $n_0 \geq 1$  such that  $a_n \leq C b_n$  and  $b_n \leq C' a_n$  for  $n \geq n_0$ .

## 2 Basic setup

We consider a general setting of many supervised learning problems. Let  $Y \in \mathcal{Y} \subset \mathbb{R}$  be a real-valued response variable and  $\mathbf{X} = (X_1, \dots, X_d)^\top$  be  $d$ -dimensional independent variables with values in a compact support  $\mathcal{X} \subset \mathbb{R}^d$ . Without loss of generality, we let  $\mathcal{X} = [0, 1]^d$ . Let  $(\mathbf{X}_i^\top, Y_i)^\top, i = 1, \dots, n$  be i.i.d. samples (a training set of  $n$  examples) drawn from the distribution of  $(\mathbf{X}^\top, Y)^\top$ . We consider the mapping  $f : \mathcal{X} \rightarrow \mathbb{R}$ . Our goal is to estimate the unknown regression function  $f(\mathbf{x})$  using sparse deep neural networks from the training set.

Let  $\mu : \mathcal{X} \times \mathcal{Y} \rightarrow [0, 1]$  be a Borel probability measure of  $(\mathbf{X}^\top, Y)^\top$ . For every  $\mathbf{x} \in \mathcal{X}$ , let  $\mu(y|\mathbf{x})$  be the conditional (w.r.t.  $\mathbf{x}$ ) probability measure of  $Y$ . Let  $\mu_X$  be the marginal probability measure of  $\mathbf{X}$ . For any  $1 \leq p \leq \infty$ , let  $\mathcal{L}^p(\mathcal{X}) = \{f : \mathcal{X} \rightarrow \mathbb{R}, f \text{ is Lebesgue measurable on } \mathcal{X} \text{ and } \|f\|_{L^p} < \infty\}$ , where  $\|f\|_{L^p} = (\int_{\mathbf{x} \in \mathcal{X}} |f(\mathbf{x})|^p d\mathbf{x})^{1/p}$  for  $1 \leq p < \infty$ , and  $\|f\|_{L^\infty} = \|f\|_\infty = \sup_{\mathbf{x} \in \mathcal{X}} |f(\mathbf{x})|$ . For  $1 \leq p < \infty$ , denote

$\|f\|_p = (\int_{\mathbf{x} \in \mathcal{X}} |f(\mathbf{x})|^p d\mu_{\mathcal{X}}(\mathbf{x}))^{1/p}$  and  $\|f\|_{p,n} = (n^{-1} \sum_{i=1}^n |f(\mathbf{X}_i)|^p)^{1/p}$ . Let  $\rho : \mathbb{R} \times \mathcal{Y} \rightarrow \mathbb{R}$  be a loss function. The true target function  $f_0$  is defined as

$$f_0 = \arg \min_{f \in \mathcal{L}^p(\mathcal{X})} \mathcal{E}(f), \text{ where } \mathcal{E}(f) = \int_{\mathcal{X} \times \mathcal{Y}} \rho(f(\mathbf{x}), y) d\mu(\mathbf{x}, y). \quad (1)$$

Next, we introduce the Korobov spaces, in which the functions need to satisfy a certain smoothness condition. The partial derivatives of  $f$  with multi-index  $\mathbf{k} = (k_1, \dots, k_d)^\top \in \mathbb{N}^d$  is given as  $D^{\mathbf{k}} f = \frac{\partial^{|\mathbf{k}|_1} f}{\partial x_1^{k_1} \dots \partial x_d^{k_d}}$ , where  $\mathbb{N} = \{0, 1, 2, \dots, \}$  and  $|\mathbf{k}|_1 = \sum_{j=1}^d k_j$ .

**Definition 1.** For  $2 \leq p \leq \infty$ , the Sobolev spaces of mixed second derivatives (also called Korobov spaces)  $W^{2,p}(\mathcal{X})$  are define by

$$W^{2,p}(\mathcal{X}) = \{f \in \mathcal{L}^p(\mathcal{X}) : D^{\mathbf{k}} f \in \mathcal{L}^p(\mathcal{X}), |\mathbf{k}|_\infty \leq 2\}, \text{ where } |\mathbf{k}|_\infty = \max_{j=1, \dots, d} k_j.$$

**Assumption 1.** We assume that  $f_0 \in W^{2,p}(\mathcal{X})$ , for a given  $2 \leq p \leq \infty$ .

**Remark 1.** Assumption 1 imposes a smoothness condition on the target function (Bungartz & Griebel, 2004; Griebel, 2006; Montanelli & Du, 2019). The Korobov spaces  $W^{2,p}(\mathcal{X})$  are subsets of the regular Sobolev spaces defined as  $S^{2,p}(\mathcal{X}) = \{f \in \mathcal{L}^p(\mathcal{X}) : D^{\mathbf{k}} f \in \mathcal{L}^p(\mathcal{X}), |\mathbf{k}|_1 \leq 2\}$  assumed in the traditional nonparametric regression setting (Wasserman, 2006). For instance, when  $d = 2$ ,  $|\mathbf{k}|_\infty = \max(k_1, k_2) \leq 2$  implies  $|\mathbf{k}|_1 = k_1 + k_2 \leq 4$ . If  $f \in W^{2,p}(\mathcal{X})$ , it needs to satisfy

$$\frac{\partial f}{\partial x_j}, \frac{\partial^2 f}{\partial x_j^2}, \frac{\partial^2 f}{\partial x_1 \partial x_2}, \frac{\partial^3 f}{\partial x_1^2 \partial x_2}, \frac{\partial^3 f}{\partial x_1 \partial x_2^2}, \frac{\partial^4 f}{\partial x_1^2 \partial x_2^2} \in \mathcal{L}^p(\mathcal{X}).$$

If  $f \in S^{2,p}(\mathcal{X})$ , it needs to satisfy  $\frac{\partial f}{\partial x_j}, \frac{\partial^2 f}{\partial x_j^2}, \frac{\partial^2 f}{\partial x_1 \partial x_2} \in \mathcal{L}^p(\mathcal{X})$ . It is worth noting that no nonparametric regression methods can avoid the ‘‘curse of dimensionality’’ if the target function belongs to the regular Sobolev spaces. Functions in the Korobov spaces need to be smoother than those in the regular Sobolev spaces, and many popular structured nonparametric models satisfy this condition (see Griebel, 2006). Note that when  $d = 1$

(one-dimensional nonparametric regression), the Korobov and the Sobolev spaces are the same, i.e., if  $f \in W^{2,p}(\mathcal{X})$  or  $f \in S^{2,p}(\mathcal{X})$ , it needs to satisfy  $\frac{\partial f}{\partial x_1}, \frac{\partial^2 f}{\partial x_1^2} \in \mathcal{L}^p(\mathcal{X})$ .

Below, we provide several examples of regression functions that belong to the Korobov space given in Definition 1, so they satisfy the condition in Assumption 1. These regression models are popularly used in the non- and semi-parametric regression literature. Let  $\mathbf{x} = (x_1, x_2, \dots, x_d)^\top$ .

**Example 1. Additive model** (Stone, 1985) is defined as  $f_0(\mathbf{x}) = \sum_{j=1}^d f_j(x_j)$ , where  $f_j(\cdot)$  is an unknown but smooth function of the  $j^{\text{th}}$  covariate, for  $j = 1, \dots, d$ . In the literature, to ensure nonparametric estimators of  $f_j(\cdot)$  have a good convergence rate, it requires a smoothness condition on each univariate function  $f_j(\cdot)$ , such as  $D^2 f_j \in \mathcal{L}^p(\mathcal{X})$ , i.e., the second derivative of  $f_j(\cdot)$  exists and is integrable, then the regression function  $f_0 \in W^{2,p}(\mathcal{X})$ , satisfying Assumption 1.

**Example 2. Functional ANOVA model** (Stone, Hansen, Kooperberg, & Truong, 1997) consists of the main and interaction effect terms. It is typically expressed as

$$f_0(\mathbf{x}) = \sum_{j=1}^d f_j(x_j) + \sum_{i \neq j} f_{jj'}(x_{j'}, x_j),$$

where  $f_j$  are unknown but smooth functions for the main effects and  $f_{jj'}$  are unknown functions for the second-order interaction effects. When the univariate functions  $f_j$  and the bivariate functions  $f_{jj'}$  satisfy the smoothness conditions such that  $D^2 f_j \in \mathcal{L}^p(\mathcal{X})$  and  $D^{\mathbf{k}} f_{jj'} \in \mathcal{L}^p(\mathcal{X})$  for  $|\mathbf{k}|_\infty = \max(k_1, k_2) \leq 2$ , where  $\mathbf{k} = (k_1, k_2)^\top$ , the regression function  $f_0 \in W^{2,p}(\mathcal{X})$ , satisfying Assumption 1.

**Example 3. Sparse tensor decomposition model** (Schmidt-Hieber, 2020) assumes that the regression function has the form

$$f_0(\mathbf{x}) = \sum_{\ell=1}^L \alpha_\ell \prod_{j=1}^d f_{j\ell}(x_j),$$



for fixed  $L$ , real coefficients  $\alpha_\ell$  and univariate functions  $f_{j\ell}$ . When the unknown univariate functions  $f_{j\ell}$  satisfy the smoothness condition such that  $D^2 f_{j\ell} \in \mathcal{L}^p(\mathcal{X})$ , the regression function  $f_0 \in W^{2,p}(\mathcal{X})$ , satisfying Assumption 1.

**Assumption 2.** For any  $y \in \mathcal{Y}$ , the loss function  $\rho(\cdot, y)$  is convex and it satisfies the Lipschitz property such that there exists a constant  $0 < C_\rho < \infty$ , for almost every  $(\mathbf{x}, y) \in \mathcal{X} \times \mathcal{Y}$ ,  $|\rho(f_1(\mathbf{x}), y) - \rho(f_2(\mathbf{x}), y)| \leq C_\rho |f_1(\mathbf{x}) - f_2(\mathbf{x})|$ , for any  $f_1, f_2 \in \mathcal{F}$ , where  $\mathcal{F}$  is a neural network space given in Section 4.

**Remark 2.** The above Lipschitz assumption is satisfied by many commonly used loss functions. Several examples are provided below.

**Example 4.** *Huber loss* is popularly used for robust regression, and it is defined as

$$\rho(f(\mathbf{x}), y) = \begin{cases} 2^{-1}(y - f(\mathbf{x}))^2 & \text{if } |f(\mathbf{x}) - y| \leq \delta \\ \delta|y - f(\mathbf{x})| - \delta^2/2 & \text{if } |f(\mathbf{x}) - y| > \delta \end{cases}. \quad (2)$$

It satisfies Assumption 2 with  $C_\rho = \delta$ .

**Example 5.** *Quantile loss* is another popular loss function for robust regression, and it is defined as

$$\rho(f(\mathbf{x}), y) = (y - f(\mathbf{x}))(\tau - I\{y - f(\mathbf{x}) \leq 0\}) \quad (3)$$

for  $\tau \in (0, 1)$ . It satisfies Assumption 2 with  $C_\rho = 1$ .

**Example 6.** *Logistic loss* is used in logistic regression for binary responses as well as for classification. The loss function is  $\rho(f(\mathbf{x}), y) = \log(1 + e^{f(\mathbf{x})}) - yf(\mathbf{x})$  for  $y \in \{0, 1\}$ . It satisfies Assumption 2 with  $C_\rho = 2$ .

### 3 Approximation of the target function by ReLU networks

We consider feedforward neural networks which consist of a collection of input variables, one output unit, and a number of computational units (nodes) in different hidden

layers. In our setting, the  $d$ -dimensional covariates  $\mathbf{X}$  are the input variables, and the approximated function is the output unit. Each computational unit is obtained from the units in the previous layer. Following (Anthony & Bartlett, 2009), we measure the network complexity by using the depth of the network defined as the number of layers, the total number of units (nodes), and the total number of weights, which is the sum of the number of connections and the number of units. Moreover,  $\sigma : \mathbb{R} \rightarrow \mathbb{R}$  is an activation function which is chosen by practitioners. In this paper, we use the rectified linear unit (ReLU) function given as  $\sigma(x) = \max(0, x)$ .

Our goal is to propose a ReLU network estimator for the regression function (1) obtained via the regularized ERM. We are also interested in studying whether the ReLU estimator can break the “curse of dimensionality”, when the target function satisfies the condition given in (1). Below we will first provide a reasoning why a function  $f(\cdot)$  in the Korobov space such that  $f \in W^{2,p}(\mathcal{X})$  can be well approximated by a deep ReLU network. This will provide a mathematical grounding for the construction of our sparse deep ReLU network estimator introduced in Section 4.

We present several results given in (Yarotsky, 2017) to show that for the function  $v(\mathbf{u}) = \prod_{j=1}^d u_j$  with  $\mathbf{u} \in [0, 1]^d$ , where  $\mathbf{u} = (u_1, \dots, u_d)^\top$ , it can be well approximated by a ReLU network. This result will be used to construct the ReLU network approximator for the target function  $f(\cdot)$ . Consider the “tooth” function  $g : [0, 1] \rightarrow [0, 1]$  given as  $g(u) = 2u$  for  $u < 1/2$  and  $g(u) = 2(1 - u)$  for  $u \geq 1/2$ , and the iterated functions  $g_r(u) = \underbrace{g \circ g \circ \dots \circ g}_r(u)$ . Let

$$\varphi_R(u) = u - \sum_{r=1}^R \frac{g_r(u)}{2^{2r}}.$$

It is clear that  $\varphi_R(0) = 0$ . It is shown in (Yarotsky, 2017) that for the function  $v(u) = u^2$  with  $u \in [0, 1]$ , it can be approximated by  $\varphi_R(u)$  such that

$$\|v - \varphi_R\|_\infty \leq 2^{-2R-2}.$$

Moreover, the tooth function  $g$  can be implemented by a ReLU network:  $g(u) = 2\sigma(u) - 4\sigma(u - 1/2) + 2\sigma(u - 1)$  which has 1 hidden layer and 3 computational units. Therefore,  $\varphi_R(u)$  can be constructed by a ReLU network with the depth  $R + 2$ , the computational units  $3R + 1$ , and the number of weights  $12R - 5 + 3R + 1 = 15R - 4$ .

Next, we approximate the function  $v(u_1, u_2) = u_1u_2 = 2^{-1}((u_1 + u_2)^2 - u_1^2 - u_2^2)$  for  $u_1 \in [0, 1]$  and  $u_2 \in [0, 1]$  by a ReLU network as follows. By the above results, we have  $|\varphi_R((u_1 + u_2)/2) - ((u_1 + u_2)/2)^2| \leq 2^{-2R-2}$ ,  $|2^{-2}\varphi_R(u_1) - 2^{-2}u_1^2| \leq 2^{-2}2^{-2R-2}$  and  $|2^{-2}\varphi_R(u_2) - 2^{-2}u_2^2| \leq 2^{-2}2^{-2R-2}$ . Let

$$\tilde{\varphi}_R(u_1, u_2) = 2 \left\{ \varphi_R\left(\frac{u_1 + u_2}{2}\right) - \frac{\varphi_R(u_1)}{2^2} - \frac{\varphi_R(u_2)}{2^2} \right\},$$

and  $\tilde{\varphi}_R(u_1, u_2)$  can be implemented by a ReLU network having the depth, the computational units and the number of weights being  $c_1R + c_2$ , where the constants  $c_1$  and  $c_2$  can be different for these three measures. Moreover,  $\tilde{\varphi}_R(u_1, u_2) = 0$  if  $u_1u_2 = 0$ . For all  $u_1 \in [0, 1]$  and  $u_2 \in [0, 1]$ ,

$$\begin{aligned} & |\tilde{\varphi}_R(u_1, u_2) - v(u_1, u_2)| \\ &= 2 \left| \left\{ \varphi_R\left(\frac{u_1 + u_2}{2}\right) - \frac{\varphi_R(u_1)}{2^2} - \frac{\varphi_R(u_2)}{2^2} \right\} - \left\{ \left(\frac{u_1 + u_2}{2}\right)^2 - \frac{u_1^2}{2^2} - \frac{u_2^2}{2^2} \right\} \right| \\ &\leq 2 (2^{-2R-2} + 2^{-2}2^{-2R-2} + 2^{-2}2^{-2R-2}) = 3 \cdot 2^{-2R-2}. \end{aligned} \quad (4)$$

At last, we can approximate the function  $v(\mathbf{u}) = \prod_{j=1}^d u_j$  for  $\mathbf{u} \in [0, 1]^d$  from a binary tree structure constructed based on the function  $\tilde{\varphi}_R(\cdot, \cdot)$  given in (4). The resulting network is denoted by  $\tilde{\varphi}_R(\mathbf{u})$ . It can be shown from mathematical induction (Montanelli & Du, 2019) that for any  $\mathbf{u} \in [0, 1]^d$ ,

$$|\tilde{\varphi}_R(\mathbf{u}) - v(\mathbf{u})| \leq (1 + 2 + 2^2 + \dots + 2^{\lceil \log_2 d \rceil - 1}) \cdot 3 \cdot 2^{-2R-2} \leq 3 \cdot 2^{-2R-2}(d - 1), \quad (5)$$

where  $\lceil a \rceil$  is the largest integer no greater than  $a$ . Moreover,  $\tilde{\varphi}_R(\mathbf{u}) = 0$  if  $h(\mathbf{u}) = 0$ .

The ReLU network used to approximate  $\phi_{\ell,s}(\mathbf{x})$  has depth  $\mathcal{O}(R) \times \log_2 d = \mathcal{O}(R \log_2 d)$ , the computational units  $\mathcal{O}(R) \times (d + 2^{-1}d + \dots + 2^{-\lfloor \log_2 d \rfloor + 1}d) = \mathcal{O}(Rd)$ , and the number of weights  $\mathcal{O}(Rd)$ .

For any function  $f \in W^{2,p}(\mathcal{X})$ , it has a unique expression in a hierarchical basis (Bungartz & Griebel, 2004) such that  $f(\mathbf{x}) = \sum_{0_d \leq \ell \leq \infty} \sum_{s \in I_\ell} \gamma_{\ell,s}^0 \phi_{\ell,s}(\mathbf{x})$ , where  $\phi_{\ell,s}(\mathbf{x}) = \prod_{j=1}^d \phi_{\ell_j, s_j}(x_j)$  are the tensor product piecewise linear basis functions defined on the grids  $\Omega_\ell$  of level  $\ell = (\ell_1, \dots, \ell_d)^\top$ ,  $I_\ell$  are the index sets of level  $\ell$ , and the hierarchical coefficients  $\gamma_{\ell,s}^0 \in \mathbb{R}$  are given in (A.2). We refer to Section A.1 in the Appendix for a detailed discussion on the hierarchical basis functions. Section A.1 shows that for any  $f \in W^{2,p}(\mathcal{X})$ , it can be well approximated by the hierarchical basis functions with sparse grids such that  $f(\mathbf{x}) \approx \sum_{|\ell|_1 \leq m} \sum_{s \in I_\ell} \gamma_{\ell,s}^0 \phi_{\ell,s}(\mathbf{x})$ . Then the hierarchical space with sparse grids is given as

$$V_m^{(1)} = \text{span}\{\phi_{\ell,s} : s \in I_\ell, |\ell|_1 \leq m\}.$$

We provide explicit upper and lower bounds for the dimension (cardinality) of the space  $V_m^{(1)}$  in Proposition A.2.

Based on the result given in (5), we let each  $u_j = \phi_{\ell_j, s_j}(x_j)$ , so  $\mathbf{u} = \phi_{\ell,s}(\mathbf{x}) = (\phi_{\ell_1, s_1}(x_1), \phi_{\ell_2, s_2}(x_2), \dots, \phi_{\ell_d, s_d}(x_d))$ ,  $v(\mathbf{u}) = \prod_{j=1}^d \phi_{\ell_j, s_j}(x_j) = \phi_{\ell,s}(\mathbf{x})$  and thus the hierarchical basis functions  $\phi_{\ell,s}(\mathbf{x})$  can be well approximated by the ReLU network  $\tilde{\varphi}_R$ . Then the ReLU network approximator of the unknown function  $f(\mathbf{x})$  is

$$\tilde{f}(\mathbf{x}) = \sum_{|\ell|_1 \leq m} \sum_{s \in I_\ell} \gamma_{\ell,s}^0 \tilde{\varphi}_R(\phi_{\ell,s}(\mathbf{x})) = \sum_{|\ell|_1 \leq m} \tilde{g}_\ell(\mathbf{x}). \quad (6)$$

**Assumption 3.** Let  $p_X(\mathbf{x})$  be the density function of  $\mu_X(\mathbf{x})$ . Assume that for all  $\mathbf{x} \in \mathcal{X}$ ,  $0 \leq p_X(\mathbf{x}) \leq c_\mu$  for some constant  $c_\mu \in (0, \infty)$ .

**Remark 3.** We assume the density function  $p_X(\mathbf{x})$  is upper bounded by  $c_\mu$ . This condition is easily met and is used to establish approximation error bounds.

The following proposition provides the approximation error of the approximator  $\tilde{f}(\cdot)$  obtained from the ReLU network to the true unknown function  $f(\cdot)$ .

**Proposition 1.** *For any  $f \in W^{2,p}(\mathcal{X})$ ,  $2 \leq p \leq \infty$ , under Assumption 3, one has that for  $d \geq 2$ ,*

$$\|\tilde{f} - f\|_2 \leq \left\{ (3/2)2^{-2R} + 6^{-1}c_\mu 2^{-2m} \{(2/3)(m+3)\}^{d-1} \right\} \|D^2 f\|_{L^2}.$$

*The ReLU network that is used to construct the approximator  $\tilde{f}$  has the number of computational units  $\mathcal{O}(2^m d^{\frac{3}{2}} R (2e^{\frac{m+d}{d-1}})^{d-1})$ , the number of weights  $\mathcal{O}(2^m d^{\frac{3}{2}} R (2e^{\frac{m+d}{d-1}})^{d-1})$ , and depth  $\mathcal{O}(R \log_2 d)$ .*

**Remark 4.** *From the mathematical expression (6) and the construction of  $\tilde{\varphi}_R$ , we see that the approximator  $\tilde{f}(\cdot)$  of the unknown function  $f(\cdot)$  is constructed from a sparse deep ReLU network, as the nodes on each layer are not fully connected with the nodes from the previous layer, and the depth of the network has the order of  $R \log_2 d$  which increases with  $R$ .*

**Remark 5.** *(Montanelli & Du, 2019) showed that the approximation error of the deep ReLU network can achieve accuracy  $\epsilon > 0$ . We further derive an explicit form of the bound to see how it depends on the dimension and the network complexity. In Theorem 3, we will show that  $m$  and  $R$  need to grow with the sample size  $n$  slowly at a logarithmic rate to achieve a tradeoff between bias and variance, so the depth of the ReLU network grows with  $n$  at a logarithmic rate, and the number of computational units increases with  $n$  at a polynomial rate.*

#### 4 Sparse deep ReLU network estimator

In this section, we introduce the Sparse Deep ReLU Network estimator (SDRN) for the regression function (1).

#### 4.1 SDRN architecture

Our SDRN is constructed based on 3 subnetworks given in Figures 1-4 obtained from 3 steps presented as follows. Step 4 gives the output as a weighted linear combination of the network nodes. Specifically, Step 1 generates subnetwork 1 consisting of fully-connected feedforward neural networks. step 2 builds a sparse network (subnetwork 2) as a simple linear combination of the subnetworks from Step 1. Step 3 obtains the network nodes in the last hidden layer constructed from a binary tree. In Step 4, the output is obtained from a linear combination of the network nodes obtained in Step 3. Our considered SDRN can go deeper with fewer parameters to well approximate a smooth function as discussed in Section 3, and it can overcome the overfitting problem (Srivastava et al., 2014) encountered by the conventional FNNs.

**Step 1:** for any input  $u \in [0, 1]$ , we first generate a fully-connected feedforward neural network with  $r$  hidden layers and 3 nodes in each layer, denoted as

$$g_r(u, \boldsymbol{\theta}_r) = \sigma(\boldsymbol{\theta}_{r1} \sigma(\boldsymbol{\theta}_{r-1,1} \cdots \sigma(\boldsymbol{\theta}_{21} \sigma(\boldsymbol{\theta}_{11} u + \boldsymbol{\theta}_{10}) + \boldsymbol{\theta}_{20}) + \cdots \boldsymbol{\theta}_{r-1,0}) + \boldsymbol{\theta}_{r0}),$$

where  $\boldsymbol{\theta}_r = \text{vec}(\boldsymbol{\theta}_{10}, \boldsymbol{\theta}_{11}, \dots, \boldsymbol{\theta}_{r0}, \boldsymbol{\theta}_{r1})$ , in which the elements  $\boldsymbol{\theta}_{j1}$  are  $3 \times 3$  matrices for  $2 \leq j \leq r$ , while the element  $\boldsymbol{\theta}_{11}$  and  $\boldsymbol{\theta}_{j0}$ , for  $1 \leq j \leq r$ , are  $3 \times 1$  vectors. We further introduce a ReLU neural network  $\varphi_R(u, \boldsymbol{\theta}, \boldsymbol{\eta})$  constructed by  $g_r(u, \boldsymbol{\theta}_r)$ ,  $r = 1, \dots, R$ , given by  $\varphi_R(u, \boldsymbol{\theta}, \boldsymbol{\eta}) = \eta_0 u + \sum_{r=1}^R \boldsymbol{\eta}_r^\top g_r(u, \boldsymbol{\theta}_r)$ , where  $\boldsymbol{\eta}_r = 2^{-2r} \tilde{\boldsymbol{\eta}}$ ,  $\boldsymbol{\eta} = \{\eta_0, \tilde{\boldsymbol{\eta}}^\top\}^\top$  is a 4-dimensional vector and  $\boldsymbol{\theta} = \text{vec}(\boldsymbol{\theta}_{10}, \boldsymbol{\theta}_{11}, \dots, \boldsymbol{\theta}_{R0}, \boldsymbol{\theta}_{R1})$  is a  $(12R - 6)$ -dimensional vector. This network structure is depicted in Figure 1. We denote  $\varphi_R(u, \boldsymbol{\theta}, \boldsymbol{\eta})$  as Sub1.

**Step 2:** for any two-dimensional inputs  $u_1, u_2 \in [0, 1]^2$ , based on the ReLU network Sub1, we build a sparse ReLU network  $\tilde{\varphi}_R(u_1, u_2, \boldsymbol{\theta}, \boldsymbol{\eta}, \boldsymbol{\omega}) = \omega_1 \varphi_R(u_1, \boldsymbol{\theta}, \boldsymbol{\eta}) + \omega_2 \varphi_R(u_2, \boldsymbol{\theta}, \boldsymbol{\eta}) + \omega_3 \varphi_R((u_1 + u_2)/2, \boldsymbol{\theta}, \boldsymbol{\eta})$ , where  $\boldsymbol{\omega} = (\omega_1, \omega_2, \omega_3)^\top$ . The corresponding network is shown in Figure 2 and is denoted as Sub2.

**Step 3:** for any  $d$ -dimensional inputs  $\mathbf{u} \in [0, 1]^d$ , where  $\mathbf{u} = (u_1, u_2, \dots, u_d)^\top$ , we construct the sub-ReLU neural network  $\tilde{\varphi}_R(\mathbf{u}, \boldsymbol{\theta}, \boldsymbol{\eta}, \boldsymbol{\omega})$  based on a binary tree structure.

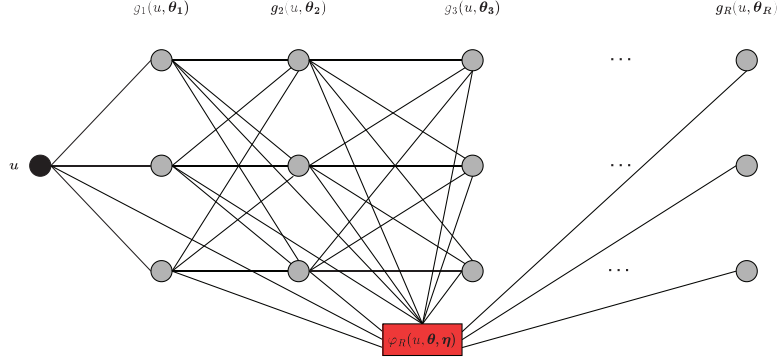


Figure 1: The construction of the function  $\varphi_R(u, \theta, \eta)$  by a ReLU network, denoted as Sub1.

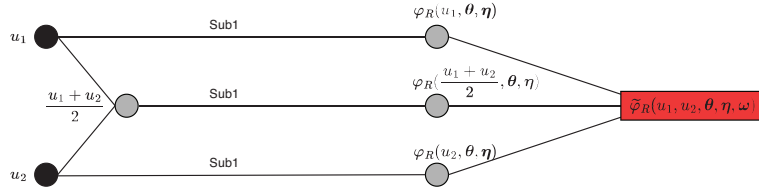


Figure 2: The construction of  $\tilde{\varphi}_R(u_1, u_2, \theta, \eta, \omega)$  from the Sub1's, denoted as Sub2.

This involves using Sub2 to integrate pairs of nodes from the preceding layer. Figure 3 shows the construction of  $\tilde{\varphi}_R(\mathbf{u}, \theta, \eta, \omega)$ , clearly illustrating that  $\tilde{\varphi}_R(\mathbf{u}, \theta, \eta, \omega)$  is a ReLU neural network with sparse connections. We denote  $\tilde{\varphi}_R(\mathbf{u}, \theta, \eta, \omega)$  as Sub3.

**Step 4:** with  $d$ -dimensional inputs  $\mathbf{x} = (x_1, x_2, \dots, x_d)$ , letting  $u_j = \phi_{\ell_j, s_j}(x_j)$  for  $1 \leq j \leq d$ , and  $\mathbf{u} = \phi_{\ell, \mathbf{s}} = (\phi_{\ell_1, s_1}(x_1), \dots, \phi_{\ell_d, s_d}(x_d))^T$ , then the output from the SDRN is built based on the linear combination of all sub-ReLU networks  $\tilde{\varphi}_R(\phi_{\ell, \mathbf{s}}, \theta, \eta, \omega)$ ,

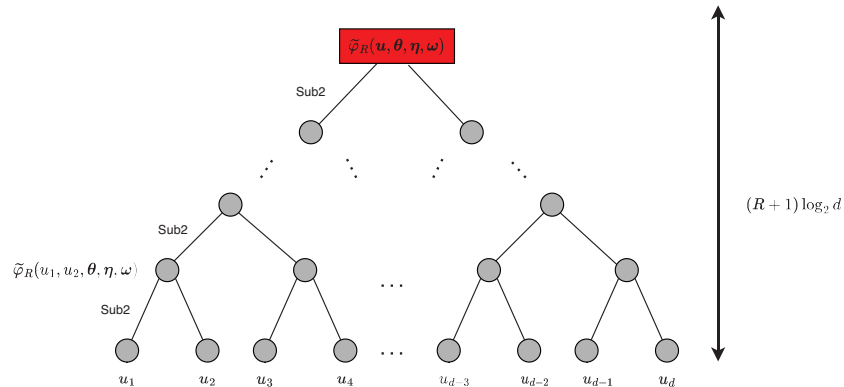


Figure 3: The construction of  $\tilde{\varphi}_R(\mathbf{u}, \theta, \eta, \omega)$  from the Sub2's, denoted as Sub3.

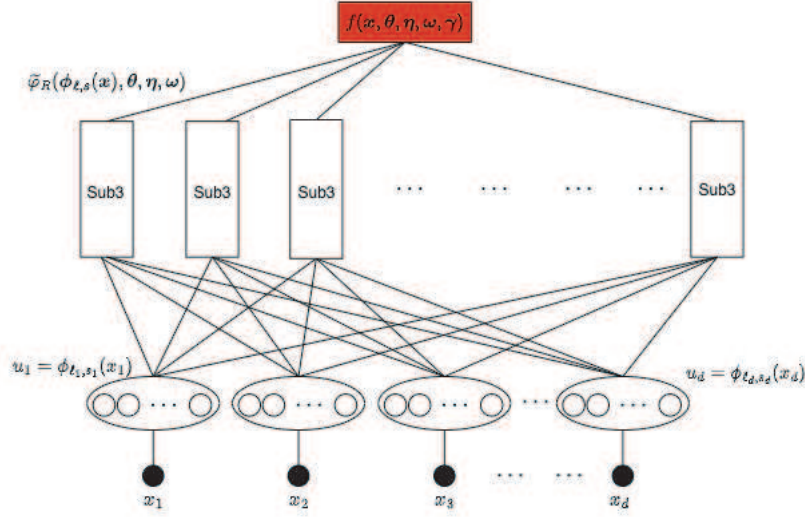


Figure 4: The construction of  $f(x, \theta, \eta, \omega, \gamma)$  from the Sub3's.

and can be expressed as

$$f(x, \theta, \eta, \omega, \gamma) = \sum_{|\ell|_1 \leq m} \sum_{s \in I_\ell} \gamma_{\ell, s} \tilde{\varphi}_R(\phi_{\ell, s}, \theta, \eta, \omega)$$

, where  $\gamma = \{\gamma_{\ell, s} : s \in I_\ell, |\ell|_1 \leq m\}^\top$ , Figure 4 shows the resulting network architecture.

We provide a pseudocode for constructing the SDRN based on the previous 4 steps in Algorithm 1.

## 4.2 SDRN estimator

We denote the vector of the whole parameters in  $f(x, \theta, \eta, \omega, \gamma)$  as  $\Theta = (\theta^\top, \eta^\top, \omega^\top, \gamma^\top)^\top$ . Then the SDRN estimator can be written as  $f(x, \Theta) = f(x, \theta, \eta, \omega, \gamma)$ . Since the ReLU network function  $\tilde{f}$  in (6) is constructed in the same way as above, there exists a set of parameters  $\Theta^0 = (\theta^{0\top}, \eta^{0\top}, \omega^{0\top}, \gamma^{0\top})^\top$  such that  $\tilde{f}$  can be written  $\tilde{f}(x, \Theta^0)$ .



---

**Algorithm 1** Pseudocode to construct SDRN, refer to Section 4.1 for detailed explanation. Let  $\mathbf{u} = \phi_{\ell,s}(\mathbf{x}) = (\phi_{l_1,s_1}(x_1), \phi_{l_2,s_2}(x_2), \dots, \phi_{l_d,s_d}(x_d))$  be a  $d$ -dimensional vector and denote the last element in  $\mathbf{u}$  as  $\mathbf{u}[-1]$ , and  $u, u_1, u_2$  are scalars.

---

**Require:** Input  $\mathbf{x}_{n \times d}$ :  $d$ -dimensional data with sample size  $n$

**Require:**  $m$ : control the number of basis functions

**Require:**  $\Theta = (\boldsymbol{\theta}^\top, \boldsymbol{\eta}^\top, \boldsymbol{\omega}^\top, \boldsymbol{\gamma}^\top)^\top$ : parameter vector

$R = 3 \max(\lfloor 0.2 \log_2 n \rfloor, m)$  (number of hidden layers in  $\varphi_R(u, \boldsymbol{\theta}, \boldsymbol{\eta})$ )

**function**  $\varphi_R(u, \boldsymbol{\theta}, \boldsymbol{\eta})$  (Sub1)

$s_r \leftarrow \eta_0 \cdot u$  (Initialize the starting sum value)

$h_r \leftarrow u$  (layer's input)

**for**  $r$  from 1 to  $R$  **do** (Iterate from the first hidden layer to the last)

$g_r \leftarrow \sigma(\boldsymbol{\theta}_{r1} \cdot h_r + \boldsymbol{\theta}_{r0})$  (Compute the layer's output)

$s_r \leftarrow s_r + \boldsymbol{\eta}_r^\top \cdot g_r$  (Add the weighted output of this layer)

$h_r \leftarrow g_r$  (Update layer's input for the next layer)

**end for**

**return**  $s_r$

**end function**

**function**  $\tilde{\varphi}_R(u_1, u_2, \boldsymbol{\theta}, \boldsymbol{\eta}, \boldsymbol{\omega})$  (Sub2)

**return**  $\omega_1 \varphi_R(u_1, \boldsymbol{\theta}, \boldsymbol{\eta}) + \omega_2 \varphi_R(u_2, \boldsymbol{\theta}, \boldsymbol{\eta}) + \omega_3 \varphi_R(\frac{u_1+u_2}{2}, \boldsymbol{\theta}, \boldsymbol{\eta})$

**end function**

**function**  $\tilde{\varphi}_R(\mathbf{u}, \boldsymbol{\theta}, \boldsymbol{\eta}, \boldsymbol{\omega})$  (Sub3: binary tree structure)

$p \leftarrow \text{length}(\mathbf{u})$  ( $p$  represents the number of elements in  $\mathbf{u}$ )

**while**  $p \geq 2$  **do**

$\mathbf{u}' \leftarrow []$  (Initialize an empty vector  $\mathbf{u}'$  to store elements in next layer)

**for**  $j$  from 1 to  $\lfloor p/2 \rfloor$  **do**

$\mathbf{u}'[j] \leftarrow \tilde{\varphi}_R(\mathbf{u}[2j-1], \mathbf{u}[2j], \boldsymbol{\theta}, \boldsymbol{\eta}, \boldsymbol{\omega})$

(Call Sub2 to combine the pair of elements for the next layer  $\mathbf{u}'$ )

**end for**

**if**  $p$  is odd **then**

$\mathbf{u}' \leftarrow [\mathbf{u}' \quad \mathbf{u}[-1]]$

(If there's an unpaired element left, carry it over to  $\mathbf{u}'$ )

**end if**

$\mathbf{u} \leftarrow \mathbf{u}'$  (Replace  $\mathbf{u}$  with the new layer, continue to the next layer)

$p \leftarrow \text{length}(\mathbf{u})$  (Update  $p$  to the current length of  $\mathbf{u}$ )

**end while**

**return**  $\mathbf{u}$

**end function**

**Output**  $f(\mathbf{x}, \boldsymbol{\theta}, \boldsymbol{\eta}, \boldsymbol{\omega}, \boldsymbol{\gamma}) \leftarrow \sum_{|\ell_1| \leq m} \sum_{s \in I_\ell} \gamma_{\ell,s} \tilde{\varphi}_R(\phi_{\ell,s}(\mathbf{x}), \boldsymbol{\theta}, \boldsymbol{\eta}, \boldsymbol{\omega})$

(Call Sub3 for each  $\phi_{\ell,s}(\mathbf{x})$ , then linearly combine  $\tilde{\varphi}_R(\phi_{\ell,s}(\mathbf{x}), \boldsymbol{\theta}, \boldsymbol{\eta}, \boldsymbol{\omega})$ )

---

Define the ReLU network class as

$$\mathcal{F}(R, m, B_0, B_1) = \left\{ f : \mathcal{X} \rightarrow \mathbb{R}, f(\mathbf{x}, \Theta) = \sum_{|\ell_1| \leq m} \sum_{s \in I_\ell} \gamma_{\ell, s} \tilde{\varphi}_R(\phi_{\ell, s}(\mathbf{x}), \theta, \eta, \omega), \right. \\ \left. \gamma_{\ell, s} \in \mathbb{R}, \|f\|_\infty \leq B_0, |\Theta|_2 \leq B_1 \right\}, \quad (7)$$

with  $B_0 \geq \max(\|f_0\|_\infty, \|\tilde{f}\|_\infty)$  and  $B_1 \geq |\Theta^0|_2$ . Then  $\tilde{f} \in \mathcal{F}(R, m, B_0, B_1)$ .

Define the empirical risk as  $\mathcal{E}_n(f; \Theta) = n^{-1} \sum_{i=1}^n \rho(f(\mathbf{X}_i, \Theta), Y_i)$ , and the regularized empirical risk as  $\mathcal{E}_n^P(f; \Theta) = n^{-1} \sum_{i=1}^n \rho(f(\mathbf{X}_i, \Theta), Y_i) + 2^{-1} \lambda \Theta^\top \Theta$ , where  $\lambda > 0$  is a tuning parameter for the  $L_2$  (ridge) penalty. The  $L_2$  penalty is often used to prevent over-fitting. When  $\lambda = 0$ , the regularized empirical risk is reduced to be the empirical risk. Then, the penalized SDRN estimator  $\hat{f}$  of  $f_0$  satisfies

$$\mathcal{E}_n^P(\hat{f}; \hat{\Theta}) \leq \min_{f \in \mathcal{F}(R, m, B_0, B_1)} \{\mathcal{E}_n^P(f; \Theta)\} + \varpi_n, \quad (8)$$

where  $\hat{f}(\mathbf{x}) = f(\mathbf{x}, \hat{\Theta})$ , and  $\varpi_n = o(1)$  satisfying a condition given in Theorem 1. Note that the penalized SDRN estimator  $\hat{f}$  obtained from (8) does not need to be the global minimizer of the objective function  $\mathcal{E}_n^P(f; \Theta)$ ; it can be any local solution such that the difference of the objective function values evaluated at the local solution and the global minimizer is bounded by a small term  $\varpi_n$ . We adopt the Adam algorithm given in (Kingma & Ba, 2015) for obtaining the estimate of  $\Theta$ . This algorithm considers first-order gradient-based optimization, and it is straightforward to implement and has little memory requirements. We use the default settings for the hyperparameters used in the Adam algorithm given in (Kingma & Ba, 2015).

## 5 Theory

For a given estimator  $\hat{f}$ , we define the overall error as  $\mathcal{E}(\hat{f}) - \mathcal{E}(f_0)$ , which is used to measure how close the estimator  $\hat{f}$  to the true target function  $f_0$ . Let

$$f^* = \arg \min_{f \in \mathcal{F}(R, m, B_0, B_1)} \mathcal{E}(f), \text{ where } \mathcal{E}(f) = \int_{\mathcal{X} \times \mathcal{Y}} \rho(f(\mathbf{x}, \Theta), y) d\mu(\mathbf{x}, y). \quad (9)$$

Then the overall error of the estimator  $\hat{f}$  can be split into the approximation error  $\mathcal{E}(f^*) - \mathcal{E}(f_0)$  and the sampling error  $\mathcal{E}(\hat{f}) - \mathcal{E}(f^*)$  such that

$$\underbrace{\mathcal{E}(\hat{f}) - \mathcal{E}(f_0)}_{\text{overall error}} = \underbrace{\mathcal{E}(f^*) - \mathcal{E}(f_0)}_{\text{approximation error}} + \underbrace{\mathcal{E}(\hat{f}) - \mathcal{E}(f^*)}_{\text{estimation error}}.$$

We will establish the upper bounds for the approximation error and the estimation error, respectively, as follows.

We introduce the following Bernstein condition that is required for obtaining the probability bound for the estimation error of our SDRN estimator.

**Assumption 4.** *There exists a constant  $0 < a_\rho < \infty$  such that*

$$a_\rho \|f - f^*\|_2^2 \leq \mathcal{E}(f) - \mathcal{E}(f^*) \quad (10)$$

for any  $f \in \mathcal{F}(R, m, B_0, B_1)$ .

**Remark 6.** *The Bernstein condition given in (10) for Lipschitz loss functions is used in the literature in order to establish probability bounds of estimators obtained from empirical risk minimization (Alquier, Cottet, & Lecué, 2019). A more general form is  $a_\rho \|f - f^*\|_2^{2\kappa} \leq \mathcal{E}(f) - \mathcal{E}(f^*)$  for some  $\kappa \geq 1$ . The parameter  $\kappa$  can affect the estimator's rate of convergence. For proof convenience, we let  $\kappa = 1$  which is satisfied by many commonly used loss functions. We will give a detailed discussion on this Bernstein condition, and will present different examples in Section 6.*

**Remark 7.** From the Lipschitz condition given in Assumption 2, we have that there exists a constant  $0 < M_\rho < \infty$  such that  $|\rho(f(\mathbf{x}), y)| \leq M_\rho$ , for almost every  $(\mathbf{x}, y) \in \mathcal{X} \times \mathcal{Y}$  and any  $f \in \mathcal{F}(R, m, B_0, B_1)$ .

Another condition is given below and it is used for controlling the approximation error from the ReLU networks.

**Assumption 5.** There exists a constant  $0 < b_\rho < \infty$  such that

$$\mathcal{E}(f) - \mathcal{E}(f_0) \leq b_\rho \|f - f_0\|_2^2 \quad (11)$$

for any  $f \in \mathcal{F}(R, m, B_0, B_1)$ .

**Remark 8.** Assumption 5 is introduced for controlling the approximation error  $\mathcal{E}(f^*) - \mathcal{E}(f_0)$ , but it is not required for establishing the upper bound of the sampling error  $\mathcal{E}(\hat{f}) - \mathcal{E}(f^*)$ . The approximation error  $\mathcal{E}(f^*) - \mathcal{E}(f_0)$  can be well controlled based on the result from Proposition 1 together with Assumption 5. Without this assumption, the approximation error will have a slower rate. Assumption 5 is satisfied by the quadratic, logistic, quantile and Huber loss functions under mild conditions. More discussions on this assumption will be provided in Section 6.

Under Condition (11) given in Assumption 5, by the definition of  $f^*$  given in (9) and Proposition 1, the approximation error

$$\mathcal{E}(f^*) - \mathcal{E}(f_0) \leq \mathcal{E}(\tilde{f}) - \mathcal{E}(f_0) \leq b_\rho \|\tilde{f} - f_0\|_2^2.$$

Since  $f_0$  satisfies Assumption 1, then  $\|D^2 f_0\|_{L^2} \leq C_f$  for some constant  $C_f \in (0, \infty)$ . Next proposition presents an upper bound for the approximation error when the unknown function  $f_0$  is approximated by the SDRN obtained from the ERM in (9).

**Proposition 2.** Under Assumptions 1, 3 and 5, and  $R \geq m$  and  $d \geq 2$ , one has

$$\mathcal{E}(f^*) - \mathcal{E}(f_0) \leq \zeta_{m,d},$$

where

$$\zeta_{m,d} = 4^{-1}b_\rho(3 + c_\mu/3)^2 2^{-4m} \{(2/3)(m+3)\}^{2(d-1)} \|D^2 f_0\|_{L^2}^2, \quad (12)$$

in which  $c_\mu$  and  $b_\rho$  are given in Assumptions 3 and 5, respectively.

Note that without Assumption 5, we obtain a looser bound for  $\mathcal{E}(f^*) - \mathcal{E}(f_0) = \mathcal{O}(\zeta_{m,d}^{1/2})$  based on the result  $\mathcal{E}(\tilde{f}) - \mathcal{E}(f_0) \leq C_\rho \|\tilde{f} - f_0\|_2$  which is directly implied from Assumption 2.

Next we establish the bound for the sampling error  $\mathcal{E}(\hat{f}) - \mathcal{E}(f^*)$ . Let  $\mathcal{N}(\delta, \mathcal{F}, \|\cdot\|_\infty)$  be the covering number, that is, the minimal number of  $\|\cdot\|_\infty$ -balls with radius  $\delta$  that covers  $\mathcal{F}$  and whose centers reside in  $\mathcal{F}$ . In the theorem below, we provide an upper bound for the estimation error  $\mathcal{E}(\hat{f}) - \mathcal{E}(f^*)$ .

**Theorem 1.** *Under Assumptions 1-4, we have that for any  $\epsilon > 0$  and  $\varpi_n + \lambda B_1^2 < (1/2)\epsilon$ ,*

$$P \left\{ \mathcal{E}(\hat{f}) - \mathcal{E}(f^*) > (3/2)\epsilon \right\} \leq \mathcal{N}(\sqrt{2}C_\rho^{-1}\epsilon/8, \mathcal{F}(R, m, B_0, B_1), \|\cdot\|_\infty) \exp(-n\epsilon/C^*)$$

, where  $C^* = 64(C_\rho^2 a_\rho^{-1} + 4M_\rho/3)$ , in which  $C_\rho, a_\rho$  and  $M_\rho$  are constants given in Assumptions 2 and 4 and Remark 7.

**Theorem 2.** *Under the same assumptions as given in Theorem 1, there exist constants  $c, C \in (0, \infty)$  such that*

$$P \left( \mathcal{E}(\hat{f}) - \mathcal{E}(f^*) > \frac{3C^*CWL \log(W)}{2n} \max\left(1, \log \frac{C^{**}n}{cWL \log(W/L)\varsigma}\right) \right) \leq \varsigma.$$

where  $C^*$  is given in Theorem 1,  $C^{**} = 16C_\rho B_0 C^{*-1}$ ,  $\varsigma \asymp \left(\frac{16C_\rho B_0}{\epsilon}\right)^{WL \log(W)} \exp\left(\frac{-n\epsilon}{C^*}\right)$ , in which the number of parameters in the sparse deep ReLU network is  $W \asymp |V_m^{(1)}| + R$  and the number of layers is  $L \asymp R \log_2 d$ .

Based on the upper bound for the estimation error given in Theorem 2, and the bound for the approximation error given in (12), we can further obtain the risk rate of

the SDRN estimator  $\widehat{f}$  presented in the following theorems.

**Theorem 3.** *Under Assumptions 1-5,  $2^m \asymp n^{1/5}$ ,  $R \asymp \log_2 n$  and  $m \leq R$ , when  $d = \mathcal{O}((\log_2 n)^{1-\kappa})$  for an arbitrary small constant  $\kappa > 0$ , then the penalized SDRN estimator  $\widehat{f}$  given in (8) with  $\varpi_n = \mathcal{O}(n^{-\frac{4}{5}+\frac{\nu}{2}}(\log_2 n)^{\frac{3\kappa}{2}+2})$  and  $\lambda = \mathcal{O}(n^{-\frac{4}{5}+\frac{\nu}{2}}(\log_2 n)^{\frac{3\kappa}{2}+2})$  has the risk rate*

$$\mathcal{E}(\widehat{f}) - \mathcal{E}(f_0) = o_p(n^{-4/5+\nu}(\log_2 n)^{-2}), \text{ for an arbitrarily small } \nu > 0.$$

*The approximation error satisfies  $\mathcal{E}(f^*) - \mathcal{E}(f_0) = o(n^{-4/5+\nu}(\log_2 n)^{-2})$ , and the estimation error satisfies  $\mathcal{E}(\widehat{f}) - \mathcal{E}(f^*) = \mathcal{O}_p(n^{-4/5+\nu/2}(\log_2 n)^{7/2-\kappa/2})$ . The ReLU network that is used to construct the estimator  $\widehat{f}$  has depth  $\mathcal{O}[\log_2 n \{\log_2(\log_2 n)\}]$ , the number of computational units  $\mathcal{O}\{(\log_2 n)^{3/2(1-\kappa)} n^{1/5+\nu/2}\}$ , and the number of weights  $\mathcal{O}\{(\log_2 n)^{3/2(1-\kappa)} n^{1/5+\nu/2}\}$ .*

**Proposition 3.** *Under the same conditions in Theorem 2, when  $d$  is fixed, then the penalized SDRN estimator  $\widehat{f}$  given in (8) with  $\varpi_n = \mathcal{O}(n^{-4/5+\nu/2}(\log_2 n)^{3\kappa/2+2})$  and  $\lambda = \mathcal{O}(n^{-4/5+\nu/2}(\log_2 n)^{3\kappa/2+2})$  has the risk rate*

$$\mathcal{E}(\widehat{f}) - \mathcal{E}(f_0) = \mathcal{O}_p(n^{-4/5}(\log_2 n)^{(d+3)\vee(2d-2)}).$$

*Moreover, the approximation error satisfies  $\mathcal{E}(f^*) - \mathcal{E}(f_0) = \mathcal{O}(n^{-4/5}(\log_2 n)^{2d-2})$ , and the estimation error satisfies  $\mathcal{E}(\widehat{f}) - \mathcal{E}(f^*) = \mathcal{O}_p(n^{-4/5}(\log_2 n)^{d+3})$ . The ReLU network that is used to construct the estimator  $\widehat{f}$  has depth  $\mathcal{O}(\log_2 n)$ , the number of computational units  $\mathcal{O}\{(\log_2 n)^d n^{1/5}\}$ , and the number of weights  $\mathcal{O}\{(\log_2 n)^d n^{1/5}\}$ .*

**Remark 9.** *We focus on deriving the optimal risk rate for the SDRN estimator of the unknown function  $f_0$  when it belongs to the Korobov space of mixed derivatives of order  $\beta = 2$ . Then the derived rate can be written as  $n^{-2\beta/(2\beta+1)}(\log_2 n)^{2d}$  when  $d$  is fixed. It is possible to derive a similar estimator for a smoother regression function that has mixed derivatives of order  $\beta > 2$  when Jacobi-weighted Korobov spaces*

(J. Shen & Wang, 2010) are considered. This can be an interesting topic for the future work.

**Remark 10.** *It is worth noting that for the classical nonparametric regression estimators such as spline estimators (Stone, 1982), the optimal minimax risk rate is  $n^{-4/(4+d)}$ , if the regression function belongs to the Sobolev spaces  $S^{2,p}(\mathcal{X})$ . This rate suffers from the curse of dimensionality as  $d$  increases.*

(Bauer & Kohler, 2019) showed that their least squares neural network estimator can achieve the rate  $n^{-2\beta/(2\beta+d^*)}$  (up to a log factor), if the regression function satisfies a  $\beta$ -smooth generalized hierarchical interaction model of order  $d^*$ . When  $\beta = 2$ , the rate is  $n^{-4/(4+d^*)}$ . The rates mentioned above require  $d$  to be fixed. (Bauer & Kohler, 2019) consider a smooth activation function, while (Schmidt-Hieber, 2020) have established a similar optimal rate for ReLU activation function.

Proposition 3 shows that when  $f_0$  belongs to the Korobov spaces  $W^{2,p}(\mathcal{X})$ , our SDRN estimator has the risk rate  $n^{-4/5}(\log_2 n)^{2d+1}$  and it achieves the optimal minimax rate (up to a log factor) as one-dimensional nonparametric regression, if the dimension  $d$  is fixed. The effect of  $d$  is passed on to a logarithm order, so the curse of dimensionality can be alleviated. When  $d$  increases with  $n$  with an order  $(\log_2 n)^{1-\kappa}$ , the risk rate is slightly slower than  $n^{-4/5}$ .

(Mao & Zhou, 2022b) derived an approximation error for deep convolutional neural networks (DCNNs) when the target function belongs to Korobov spaces, but they did not provide an estimation error. Estimators obtained from ERM have two errors: the approximation error and the estimation error. The mean squared error used to evaluate the overall performance of a machine learning estimator comes from both errors. When their approximation error is in the same order as (similar to) ours, their network size needs to be significantly larger than ours, leading to a larger estimation error. Specifically, to reach the approximation accuracy, the total number of free parameters  $\mathcal{N}$  in

their DCNNs given in equation (2.2) of (Mao & Zhou, 2022b) is

$$\mathcal{N} \leq 13385d^2(\log_2 d)^2(\log_2 N)^2N, \text{ with } N \geq 2^{16}. \quad (13)$$

By the construction of our proposed SDRN in Section 4.1, the total number of free parameters in SDRN is bounded by

$$\begin{aligned} |\Theta| &= |\gamma| + |\theta| + |\eta| + |\omega| = |V_m^{(1)}| + |\theta| + |\eta| + |\omega| \\ &\leq \sum_{|\ell|_1 \leq m} 2^{\sum_{j=1}^d \ell_j \wedge 2-d} + 12R + 1, \end{aligned} \quad (14)$$

where  $m = \lfloor 0.2 \log_2 n \rfloor$  and  $R = 3 \max(\lfloor 0.2 \log_2 n \rfloor, m)$  used in our numerical analysis. We see that our SDRN requires much fewer free parameters than DCNNs to achieve the same order of the approximation error. For example, for  $n = 2000$  and  $d = 10$ , the network size of our SDRN is bounded by 67657, while it is  $14770624 \times (\log_2 N)^2 N$  with  $N \geq 2^{16}$  for DCNNs. Since the estimation error depends on the model complexity, our SDRN has a smaller estimation error and overall better performance.

**Proposition 4.** *Under the same conditions in Theorem 3, when the sample size is sufficiently large, the lower bound for the overall error of the penalized SDRN estimator  $\hat{f}$  given in (8) is given as*

$$P\left(\mathcal{E}(\hat{f}) - \mathcal{E}(f_0) > c_1 n^{-4/5} (\log_2 n)^2 \log_2 d\right) \geq 1/100,$$

for some constant  $c_1 > 0$ .

**Remark 11.** *Proposition 4 presents a lower bound for the overall error of the SDRN estimator  $\hat{f}$ . When  $d$  is fixed, the rate of the lower bound is comparable to the upper bound rate given in Proposition 3, which is  $n^{-4/5} (\log_2 n)^{(d+3)\vee(2d-2)}$ , but it is smaller than the upper bound as one can show that  $(\log_2 n)^2 \log_2 d < (\log_2 n)^{(d+3)\vee(2d-2)}$ . Thus, our SDRN estimator achieves a nearly tight optimal risk rate.*



## 6 Discussions on Assumptions 4 and 5

We first state a general condition given in Assumption 6 presented below. We will show that if a loss function satisfies this condition, then it will satisfy Assumption 4 (Bernstein condition) and Assumption 5.

**Assumption 6.** *For all  $y \in \mathcal{Y}$ , the loss function  $\rho(\cdot, y)$  is strictly convex and it has a bounded second derivative such that  $\rho''(\cdot, y) \in [2a_\rho, 2b_\rho]$  almost everywhere, for some constants  $0 < a_\rho \leq b_\rho < \infty$ .*

Assumption 6 is satisfied by a variety of classical loss functions such as quadratic loss and logistic loss. For example, for the quadratic loss  $\rho(f(\mathbf{x}), y) = (y - f(\mathbf{x}))^2$ , clearly  $\rho''(\cdot, y) = 2$ , so  $a_\rho = b_\rho = 1$ .

Let  $f_0$  solve  $\int_{\mathcal{Y}} \rho'(f_0(\mathbf{x}), y) d\mu(y|\mathbf{x}) = 0$  and  $f_0 \in W^{2,p}(\mathcal{X})$ . Then  $f_0$  is the target function that minimizes the expected risk given in (1). Lemma 1 given below will show that Assumptions 4 and 5 are implied from Assumption 6.

**Lemma 1.** *Under Assumption 6, for any  $f \in \mathcal{F}(R, m, B_0, B_1)$ , one has  $a_\rho \|f - f^*\|_2^2 \leq \mathcal{E}(f) - \mathcal{E}(f^*)$  and  $\mathcal{E}(f) - \mathcal{E}(f_0) \leq b_\rho \|f - f_0\|_2^2$ .*

It is easy to see that the quantile and Huber loss functions do not satisfy Assumption 6. In the lemmas below we will show that under mild conditions, Assumptions 4 and 5 are satisfied by the quantile and Huber loss functions.

**Lemma 2.** *Assume that for all  $\mathbf{x} \in \mathcal{X}$ , it is possible to define a conditional density function  $\mu'(u|\mathbf{x})$  of  $Y|\mathbf{X} = \mathbf{x}$  such that  $1/C_1 \leq \mu'(u|\mathbf{x}) \leq 1/C_2$  for some  $C_1 \geq C_2 > 0$  for all  $u \in \{u \in \mathbb{R}: |u - f^*(\mathbf{x})| \leq 2B_0 \text{ or } |u - f_0(\mathbf{x})| \leq 2B_0\}$ . Then for any  $f \in \mathcal{F}(R, m, B_0, B_1)$ , the quantile loss given in (3) satisfies  $a_\rho \|f - f^*\|_2^2 \leq \mathcal{E}(f) - \mathcal{E}(f^*)$  and  $\mathcal{E}(f) - \mathcal{E}(f_0) \leq b_\rho \|f - f_0\|_2^2$  with  $a_\rho = (2C_1)^{-1}$  and  $b_\rho = (2C_2)^{-1}$ .*

**Lemma 3.** *Assume that for all  $\mathbf{x} \in \mathcal{X}$ ,  $1/c_1 \leq \mu(u + \delta|\mathbf{x}) - \mu(u - \delta|\mathbf{x}) \leq 1/c_2$  for some  $c_1 \geq c_2 > 0$  for all  $u \in \{u \in \mathbb{R}: |u - f^*(\mathbf{x})| \leq 2B_0 \text{ or } |u - f_0(\mathbf{x})| \leq 2B_0\}$ ,*

where  $\mu(u|\mathbf{x})$  is the conditional cumulative function of  $Y$  given  $Y|\mathbf{X} = \mathbf{x}$ . Then for any  $f \in \mathcal{F}(R, m, B_0, B_1)$ , the Huber loss given in (2) satisfies  $a_\rho \|f - f^*\|_2^2 \leq \mathcal{E}(f) - \mathcal{E}(f^*)$  and  $\mathcal{E}(f) - \mathcal{E}(f_0) \leq b_\rho \|f - f_0\|_2^2$  with  $a_\rho = (2c_1)^{-1}$  and  $b_\rho = (2c_2)^{-1}$ .

The proofs of Lemmas 1-3 are provided in Section A.10 of the Appendix.

**Remark 12.** We impose the upper and lower bounds for the conditional density function for  $u$  near  $f^*(\mathbf{x})$  and  $f_0(\mathbf{x})$ . The upper bounds hold because  $\mathcal{X} = [0, 1]^d$  is compact. The lower bounds ensure the density function is non-zero when  $u$  is near  $f^*$  and  $f_0$ . These mild conditions are easily satisfied.

## 7 Simulation studies

In this section, we conduct simulation studies to assess the finite-sample performance of the proposed methods.

### 7.1 Date generating process

To illustrate the methods, we generate data from the following nonlinear models:

$$\text{Model 1 : } \mathbb{E}(Y_i|X_i) = X_{i1}^{*2} X_{i2}^* + \cos(2.5(X_{i3}^* + X_{i4}^*) - 2) + 2X_{i5}^{*2} + \frac{2X_{i5}^*}{X_{i3}^{*2} + X_{i4}^{*4} + 2};$$

$$\text{Model 2 : } \mathbb{E}(Y_i|X_i) = \mathbb{P}(Y_i = 1|X_i) = \frac{e^{\eta_i}}{1 + e^{\eta_i}};$$

$$\eta_i = 4 \cos(2X_{i4}^* X_{i5}^* - X_{i2}^*) - 9X_{i3}^{*2} \sqrt{X_{i4}^* X_{i5}^* + X_{i1}^*} - 11X_{i3}^* + 12X_{i1}^{*2};$$

where  $X_i = (X_{i1}, \dots, X_{id})^\top$  is the  $d$ -dimensional vector of the covariates, for  $1 \leq i \leq n$ .

In Models 1 and 2, we let  $X_{ij}^* = \frac{5}{d} \sum_{j'=d(j-1)/5+1}^{dj/5} X_{ij'}$ , so each  $X_{ij}^*$  is the average of  $d/5$  covariates for  $1 \leq j \leq 5$ .

For Model 1, we generate the responses from  $Y_i = E(Y_i | X_i) + \epsilon_i$ , where  $\epsilon_i$  are independently generated from the standard normal distribution and Laplace distribution, respectively, for  $1 \leq i \leq n$ . For each setting, we run  $n_{rep} = 100$  replications. Let  $n = 2000, 4000$  and  $d = 5, 10, 100$ . When  $d = 5, 10$ , we generate the covariates from

$X_i \sim \mathcal{U}([0, 1]^d)$ . When  $d = 100$ , we generate the covariates from  $X_{ij} = \Phi(Z_{ij})$ , where  $\Phi$  is the cdf of the standard normal and  $Z_{ij} = F_i^\top L_j + \zeta_{ij}$ , in which  $\zeta_{ij} \sim \mathcal{N}(0, 0.5^2)$ ,  $F_i \sim \mathcal{N}(0, \Sigma)$  and  $L_j \sim \mathcal{N}(0, \Sigma)$  with  $\Sigma = \{0.5^{|k-k'|}\}_{1 \leq k, k' \leq 15}$ . We keep  $L_j$  fixed for each replication.

The nonlinear functions in Model 1 are designed based on the nonlinear patterns of the response changing with the covariates in the Boston housing data application analyzed in Section 8. Figure 5 shows the scatterplot of three simulated covariates from Model 1; we can observe similar nonlinear patterns of age, NOX, and RM in Figure 6 in Section 8.

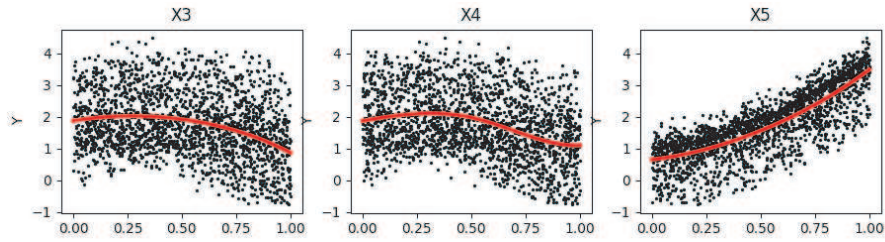


Figure 5: Scatterplot of three simulated covariates, where the red line represents the fitted mean curve by using cubic B-splines.

We evaluate the numerical results based on the same test dataset  $(y_i^*, x_i^*)$  for  $1 \leq i \leq n$  generated from our considered models. For Model 1, let  $\hat{f}(x_i^*)$  be the estimate of the regression function  $f(x_i^*)$ . We report

$$\begin{aligned} \text{average bias}^2 &= \frac{1}{n} \sum_{i=1}^n \left\{ \frac{1}{n_{rep}} \sum_{j=1}^{n_{rep}} \hat{f}(x_i^*) - f(x_i^*) \right\}^2, \\ \text{average variance} &= \frac{1}{n} \sum_{i=1}^n \left\{ \frac{1}{n_{rep}} \sum_{j=1}^{n_{rep}} \hat{f}(x_i^*)^2 - \left( \frac{1}{n_{rep}} \sum_{j=1}^{n_{rep}} \hat{f}(x_i^*) \right)^2 \right\}, \\ \text{average mse} &= \frac{1}{n} \sum_{i=1}^n \frac{1}{n_{rep}} \sum_{j=1}^{n_{rep}} \left\{ \hat{f}(x_i^*) - f(x_i^*) \right\}^2. \end{aligned}$$

For Model 2, we report the average values of square root mse (RMSE) for the estimated conditional probability, accuracy, sensitivity, specificity, precision, recall, and F1 score calculated based on the  $n_{rep} = 100$  simulation replicates. Let  $\hat{p}(x_i^*) = \hat{p}(y_i^* = 1 | x_i^*)$  be the estimated conditional probability of  $p(x_i^*) = p(y_i^* = 1 | x_i^*)$ . The average

RMSE is calculated by

$$\text{average RMSE} = \sqrt{\frac{1}{n} \sum_{i=1}^n \frac{1}{n_{rep}} \sum_{j=1}^{n_{rep}} \{\widehat{p}(x_i^*) - p(x_i^*)\}^2}.$$

## 7.2 Simulation results

We use  $m = \max(\lfloor 0.2 \log_2 n \rfloor + c, 0)$  and  $R = 3 \max(\lfloor 0.2 \log_2 n \rfloor, m)$  for the SDRN estimator, where the constant  $c$  is a tuning parameter. The choices of  $m$  and  $R$  satisfy the conditions in Theorem 3. In our procedure, we have two tuning parameters  $c$  and  $\lambda$ . The constant  $c$  determines the complexity of the neural networks, and  $\lambda$  is used in the ridge penalty term. Both of them control the fitting result. A larger value of  $c$  and a smaller value of  $\lambda$  can yield larger variance and smaller bias, while a smaller  $c$  and a larger  $\lambda$  lead to smaller variance and larger bias. We choose the optimal values for  $c$  and  $\lambda$  by minimizing the prediction errors in the test dataset.

For the large dimension setting with  $p = 100$ , to ensure robust performance, we first perform dimension reduction using PCA on the covariate matrix to reduce the high-dimensional features into lower-dimensional latent vectors, which are the leading principal components, and then use the principal components that explain the variance greater than 80% for Model 1 and 75% for Model 2 as the predictors in our regression analysis. Then the vector of the principal components would be the inputs fitting into our SDRN model, so its dimension becomes the actual dimension of the inputs for the model. Dimensionality reduction is still required for machine learning algorithms when the dimension of features is very large compared to the sample size.

Table 1 reports numerical results for the SDRN estimates from the optimal fitting with the optimal tuning parameter values for Model 1. Specifically, it shows the average mean squared error (MSE), average bias<sup>2</sup> and average variance of the SDRN estimates obtained from the quadratic and quantile ( $\tau = 0.5, 0.25$ ) loss functions, respectively, based on the 100 simulation replications. Table 1 shows that in general, the SDRN es-

Table 1: The average MSE, bias<sup>2</sup> and variance of the SDRN estimators obtained from the quadratic and quantile ( $\tau = 0.5, 0.25$ ) loss functions based on the 100 simulation replications for Model 1.

	n=2000						n = 4000					
	Normal error			Laplace error			Normal error			Laplace error		
	quadratic	$\tau = 0.5$	$\tau = 0.25$	quadratic	$\tau = 0.5$	$\tau = 0.25$	quadratic	$\tau = 0.5$	$\tau = 0.25$	quadratic	$\tau = 0.5$	$\tau = 0.25$
d = 5												
bias2	0.0125	0.0142	0.0179	0.0131	0.0144	0.0169	0.0128	0.0113	0.0119	0.0130	0.0118	0.0130
var	0.0098	0.0116	0.0124	0.0209	0.0102	0.0220	0.0052	0.0080	0.0091	0.0097	0.0072	0.0137
mse	<b>0.0223</b>	0.0257	0.0304	0.0341	<b>0.0246</b>	0.0389	<b>0.0180</b>	0.0193	0.0211	0.0226	<b>0.0190</b>	0.0267
d=10												
bias2	0.0293	0.0322	0.0352	0.0356	0.0312	0.0376	0.0262	0.0285	0.0250	0.0293	0.0252	0.0264
var	0.0167	0.0182	0.0168	0.0237	0.0161	0.0227	0.0110	0.0095	0.0126	0.0192	0.0119	0.0175
mse	<b>0.0460</b>	0.0504	0.0520	0.0592	<b>0.0472</b>	0.0603	<b>0.0372</b>	0.0379	0.0376	0.0486	<b>0.0372</b>	0.0440
d=100												
bias2	0.0352	0.0379	0.0386	0.0388	0.0372	0.0406	0.0351	0.0354	0.0360	0.0351	0.0350	0.0377
var	0.0200	0.0199	0.0206	0.0222	0.0199	0.0250	0.0155	0.0168	0.0168	0.0191	0.0164	0.0197
mse	<b>0.0552</b>	0.0578	0.0592	0.0610	<b>0.0571</b>	0.0655	<b>0.0506</b>	0.0521	0.0528	0.0542	<b>0.0514</b>	0.0575

estimates achieve a good balance between the bias<sup>2</sup> and variance at the optimal values of the tuning parameters. Moreover, we see that the MSE values decrease as the sample size increases. This corroborates with our theoretical results given in Theorem 3. The MSE values also increase gradually as the dimension  $d$  becomes larger. Our method can be applied to mean regression as well as quantile regression at any given quantile level. We observe that when the error terms are generated from a normal distribution, the SDRN estimate obtained from the quadratic loss (mean regression) has the smallest MSE, but the estimate obtained from the quantile loss at  $\tau = 0.5$  (median regression) has a comparable MSE value comparing to the estimate from the quadratic loss. However, when the errors are generated from the Laplace distribution which has heavy tails, we see that the SDRN estimate from the median regression using the quantile loss with  $\tau = 0.5$  yields obviously smaller MSE values than the estimate from the mean regression using the quadratic loss.

Next, we compare the performance of our proposed SDRN estimator with that of four other popular machine learning methods, including the fully-connected feedforward neural networks (FNN), the gradient boosted machines (GBM), the random forests (RF), and the generalized additive models (GAM). For FNN, we employ ReLU as the activation function. For GAM, a cubic regression spline basis is used. We report the results from the optimal fitting with the optimal tuning parameters minimizing the MSE

value in the test dataset. Table 2 reports the average MSE, bias<sup>2</sup> and variance for the five methods based on the 100 replicates when  $n = 2000$ ,  $d = 5, 10$ . Across all five methods, the quadratic loss and the quantile ( $\tau = 0.5$ ) loss are used for the normal and Laplace errors, respectively. We observe that our SDRN has the smallest MSE values in each case. Among all methods, the GAM method has the largest bias due to model misspecification.

We use Model 2 to illustrate the performance of the SDRN estimate for classification. Table 3 shows the average RMSE of the estimated conditional probabilities and the metrics to evaluate the classification performance, including the average values of accuracy, precision, recall, F1 score, and specificity based on 100 simulation replications for Model 2. The evaluation is performed on the test dataset, while the parameter estimates are obtained using the training dataset. The RMSE value becomes smaller when the sample size is larger, indicating that the estimated conditional probabilities are approaching the true values when the sample size is larger. This result corroborates with our theoretical property given in Proposition 3. However, the RMSE value increases slightly from  $d = 5$  to  $d = 10$ , because the effect of the dimension  $d$  is only reflected on the logarithm order given in Proposition 3. We also observe that the classification accuracy is improved as the sample size becomes larger.

We then compare the performance of the proposed SDRN with that of the four popular machine learning methods including FNN, GBM, RF and GAM for the classification task in Model 2. Table 4 reports the numerical results of the five methods obtained from the optimal fitting. The optimal values of all tuning parameters are chosen by minimizing the prediction errors in the test data. We observe that SDRN outperforms the other four methods in terms of RMSE, accuracy, recall, and F1 score. The F1 score conveys the balance between precision and recall. Overall, FNN has the second-best performance following SDRN. Its accuracy is slightly smaller than that of SDRN, but its RMSE value is significantly larger than that of SDRN when  $d = 10$ , indicating that FNN needs to have a greater network complexity than SDRN to achieve similar

Table 2: The average MSE, bias<sup>2</sup> and variance of the five methods obtained from the quadratic loss for normal error and quantile ( $\tau = 0.5$ ) loss for Laplace error based on the 100 simulation replications for Model 1 when  $n = 2000$ ,  $d = 5, 10$ .

Quadratic (Normal)						Quantile 0.5 (Laplace)				
d=5	SDRN	FNN	GBM	RF	GAM	SDRN	FNN	GBM	RF	GAM
bias2	0.0125	0.0062	0.0157	0.0386	0.1296	0.0144	0.0050	0.0238	0.0500	0.1251
var	0.0098	0.0198	0.0358	0.0523	0.0066	0.0102	0.0247	0.0327	0.0656	0.0098
mse	0.0223	0.0260	0.0514	0.0909	0.1362	0.0246	0.0298	0.0565	0.1157	0.1350
d=10	SDRN	FNN	GBM	RF	GAM	SDRN	FNN	GBM	RF	GAM
bias2	0.0293	0.0167	0.0355	0.0518	0.0712	0.0312	0.0149	0.0428	0.0544	0.0603
var	0.0167	0.0306	0.0318	0.0515	0.0136	0.0161	0.0331	0.0286	0.0726	0.0142
mse	0.0460	0.0473	0.0673	0.1033	0.0848	0.0472	0.0480	0.0714	0.1270	0.0745

Table 3: The average of RMSE, accuracy, sensitivity, precision, recall, and F1 score of the SDRN estimate based on the 100 simulation replications when  $n = 2000$  and  $n = 4000$  for Model 2.

	n=2000						n=4000					
	RMSE	Accuracy	Precision	Recall	F1	Specificity	RMSE	Accuracy	Precision	Recall	F1	Specificity
d=5	0.0617	0.9212	0.9112	0.9216	0.9163	0.9208	0.0553	0.9227	0.9156	0.9220	0.9188	0.9234
d=10	0.0667	0.8673	0.8594	0.8533	0.8562	0.8794	0.0589	0.8731	0.8613	0.8643	0.8627	0.8806
d=100	0.1838	0.7248	0.7091	0.6600	0.6832	0.7778	0.1812	0.7435	0.7347	0.6757	0.7034	0.7991

classification accuracy.

## 8 Real data application

In this section, we illustrate our proposed method by using two datasets, the Boston housing data with continuous responses and the BUPA liver disorders data with binary responses. We use the two datasets to illustrate the prediction and classification performance of our SDRN method on continuous and binary responses, respectively. Each

Table 4: The average of RMSE, accuracy, sensitivity, precision, recall, and F1 score of the five methods based on the 100 simulation replications for Model 2 when  $n = 2000$ ,  $d = 5, 10$ .

	d=5					d=10				
	SDRN	FNN	GAM	GBM	RF	SDRN	FNN	GAM	GBM	RF
RMSE	0.0617	0.0688	0.0702	0.0886	0.0896	0.0667	0.0824	0.0850	0.1020	0.1382
Accuracy	0.9212	0.9182	0.9174	0.9115	0.9135	0.8673	0.8660	0.8648	0.8610	0.8608
Precision	0.9112	0.9086	0.9072	0.8990	0.9007	0.8594	0.8603	0.8591	0.8558	0.8569
Recall	0.9216	0.9179	0.9175	0.9138	0.9165	0.8533	0.8486	0.8471	0.8416	0.8397
F1	0.9163	0.9131	0.9123	0.9063	0.9085	0.8562	0.8543	0.8530	0.8486	0.8481
Specificity	0.9208	0.9185	0.9172	0.9094	0.9108	0.8794	0.8811	0.8801	0.8777	0.8789

dataset is randomly split into 75% training data and 25% test data. The training data is used to fit the model, while the test data is used to evaluate the performance. Then, we compare our SDRN with five methods, including LM/GLM (linear model/generalized linear model), FNN, GBM, RF and GAM. For all methods, the tuning parameters are selected by 5-fold cross validations based on a grid search.

### **8.1 Boston housing data**

The Boston housing data set (Harrison Jr & Rubinfeld, 1978) contains 506 census tracts of Boston from the 1970 census. Each census tract represents one observation. Thus, there are 506 observations and 14 attributes in the dataset, where MEDV (the median value of owner-occupied homes) is the response variable. Following (Fan & Huang, 2005), seven explanatory variables are considered: CRIM (per capita crime rate by town), RM (average number of rooms per dwelling), TAX (full-value property-tax rate per USD 10,000), NOX (nitric oxides concentration in parts per 10 million), PTRATIO (pupil-teacher ratio by town), AGE (proportion of owner-occupied units built prior to 1940) and LSTAT (percentage of the lower status of the population). Since the value of the MEDV variable is censored at 50.0 (corresponding to a median price of \$50,000), we remove the 16 censored observations and use the remaining 490 observations for analysis.

For preliminary analysis of nonlinear patterns, Figure 6 shows the scatter plots of the response MEDV against each covariate with the red lines representing the fitted mean curves by using cubic B-splines. We observe that the MEDV value has a clear nonlinear changing pattern with these covariates. The MEDV value has an overall increasing pattern with RM, whereas it decreases as CRIM, NOX, PTRATIO, TAX, and LSTAT increase. The MEDV value starts decreasing slowly as AGE increases. However, when the AGE passes 60, it starts dropping dramatically.

Next, we use our SDRN method with quadratic loss to fit a mean regression of this data and compare it with LM, FNN, GBM, RF and GAM methods. Table 5 shows



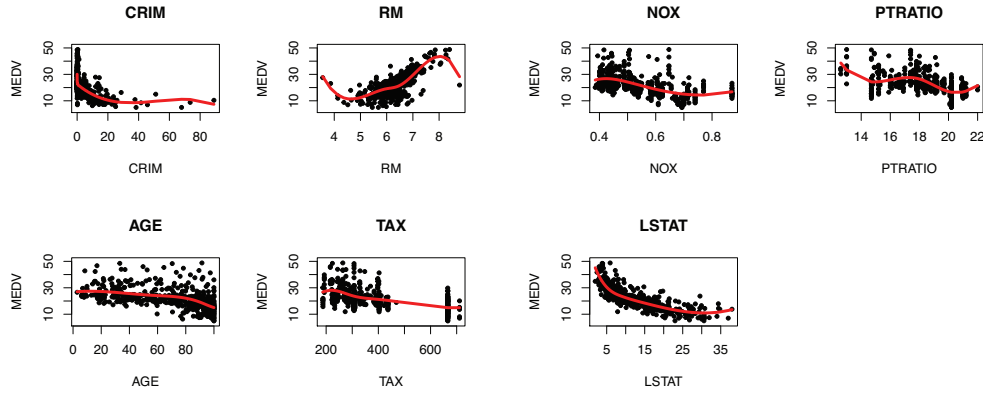


Figure 6: Scatter plot of MEDV versus each covariate, where the red line represents the fitted mean curve by using cubic B-splines.

the mean squared prediction error (MSPE) from the six methods. We observe that SDRN outperforms other methods with the smallest MSPE. The LM method has the largest MSPE, as it cannot capture the nonlinear relationships between MEDV and the covariates. GAM has the second-largest MSPE due to its restrictive additive structure without allowing interaction effects.

To explore the nonlinear patterns between MEDV and each covariate, in Figure 7 we plot the estimated mean function of MEDV versus each covariate (solid lines), and the estimated median function of MEDV versus each covariate (dashed lines), obtained from our SDRN method with the quadratic loss and the quantile ( $\tau = 0.5$ ) loss, respectively. The plots are constructed by regressing the estimated mean and median functions using cubic B-splines on each covariate.

We see that overall the fitted MEDV has a negative relationship with all covariates except RM. The estimated MEDV decreases slowly when AGE increases from 0 to 60, and then it begins to drop progressively after AGE passes 60. It suggests that the percentage of old houses in a neighborhood overall has an adverse effect on the house price, and its effect can be prominent when the percentage exceeds a certain level such as 60%. We see that the MEDV value decreases slightly when TAX increases from 200 to 300, and then its value has a steady drop when TAX increases from 300 to

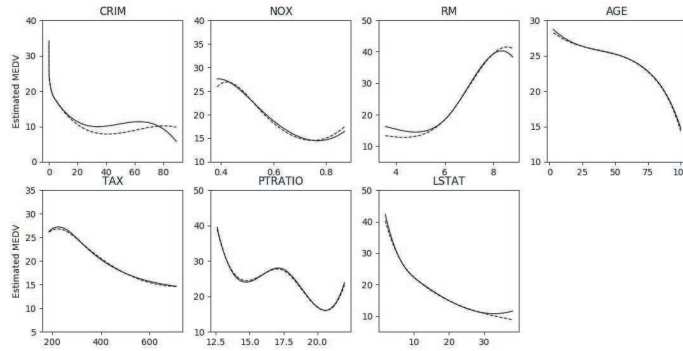


Figure 7: The estimated mean (solid lines) and median (dashed lines) curves of MEDV from SDRN against each covariate.

over 600, indicating that TAX overall has a negative impact on the house price as well. The MEDV value decreases quickly when LSTAT increases from 0 to 10, and then it levels off. This result is expected as it is difficult for the lower-status population to afford expensive houses. Moreover, the MEDV value drops gradually as the NOX level rises. This can be explained by that when the houses in a neighborhood are more expensive, this area is often less dense and has more green spaces. MEDV drops sharply as CRIM increases from 0 to 20, and it remains stable from 20 to over 80. MEDV has a high value when the PTRATIO value is small (less than 10), indicating that children in rich neighborhoods may go to private schools. The MEDV value remains stable when PTRATIO increases from 15 to 18, and then it drops steadily when PTRATIO increases from 18 to 20. Lastly, we see that overall MEDV has a steadily increasing pattern with RM. In Figure 7, we plot the estimated mean and median functions of MEDV using SDRN versus each covariate. In general, we see that the estimated mean and median functions have similar nonlinear patterns. There is a slight difference between the two curves in the tail parts for CRIM and RM. The difference may be caused by the outliers that can affect the fitting result of mean regression.

Table 5: The mean squared prediction error (MSPE) from six different methods using quadratic loss for the Boston housing data.

	<b>SDRN</b>	LM	FNN	GBM	RF	GAM
MPSE	<b>7.626</b>	15.554	7.801	7.831	9.955	12.908

## 8.2 BUPA data

The BUPA Liver Disorders dataset is available at the UCI Machine Learning Repository (Dua & Graff, 2019). It has 345 rows and 7 columns, with each row constituting the record of a single male individual. The first 5 variables are blood tests that are considered to be sensitive to liver disorders due to excessive alcohol consumption; they are mean corpuscular volume (mcv), alkaline phosphatase (alkphos), alanine aminotransferase (sgpt), aspartate aminotransferase (sgot) and gamma-glutamyl transpeptidase (gammagt). We use them as covariates. The 6th variable is the number of half-point equivalents of alcoholic beverages drunk per day. Following (McDermott & Forsyth, 2016), we dichotomize it to a binary response by letting  $Y_i = 1$  if the number of drinks is greater than 3, otherwise  $Y_i = 0$ . The 7th column in the dataset was created by BUPA researchers for training and test data selection.

We use this example to compare the performance of the classification among different methods. Table 6 shows the accuracy, precision, recall, F1, and AUC (area under the ROC curve) for the group with the number of drinks greater than 3 for the six methods with logistic loss. We see that SDRN has the largest accuracy, recall, F1, and AUC. The recall, F1, and AUC for GLM are much smaller than other methods, possibly due to model misspecification and nonlinearity of the dataset.

To explore the nonlinear patterns, Figure 8 shows the scatter plots and the fitted mean curve of the estimated conditional probabilities versus the mcv, alkphos, sgpt, sgot, and gammagt, respectively. The fitted mean curves (red lines) are drawn by regressing the estimated conditional probabilities on each predictor using cubic B-splines. We can observe the estimated conditional probability rises as mcv, gammagt increase,

Table 6: Accuracy, Precision, Recall, F1, and AUC for the group with the number of drinks greater than 3 of the BUPA data for different methods with logistic loss.

	<b>SDRN</b>	GLM	FNN	GBM	RF	GAM
Accuracy	<b>0.678</b>	0.655	0.667	0.632	0.667	0.644
Precision	<b>0.636</b>	0.652	0.618	0.561	0.643	0.583
Recall	<b>0.568</b>	0.405	0.568	0.622	0.486	0.568
F1	<b>0.600</b>	0.500	0.592	0.590	0.554	0.575
AUC	<b>0.664</b>	0.623	0.654	0.631	0.643	0.634

which suggests that the mcv and gammagt levels can be strong indicators of alcohol consumption. Both sgpt and sgot are enzymes related to liver health and seem to have similar patterns in correlation with alcohol consumption, as depicted in Figure 8. We can see the estimated conditional probability increases quickly as the level of sgpt and sgot are elevated and remain to be high as these two enzymes pass a certain value. Considering that higher levels of sgpt and sgot are associated with liver damage and excessive chronic alcohol consumption can lead to liver cell damage, it is plausible to observe a positive correlation between the levels of these two enzymes and alcohol consumption. The estimated conditional probability has a quadratic nonlinear relationship with alkphos. Abnormal (either low or high) levels of alkphos are connected to a few health problems. Low levels of alkphos indicate a deficiency in zinc and magnesium, or a rare genetic disease called hypophosphatasia, which affects bones and teeth. High levels of alkphos can be an indicator of liver disease or bone disorder.

## 9 Discussion

In this paper, we propose a sparse deep ReLU network estimator (SDRN) obtained from empirical risk minimization with a Lipschitz loss function satisfying mild conditions. Our framework can be applied to a variety of regression and classification problems in machine learning. In general, deep neural networks are effective tools for lessening the curse of dimensionality under the condition that the target functions have certain special properties. We show that our SDRN estimator achieves a fast convergence rate when

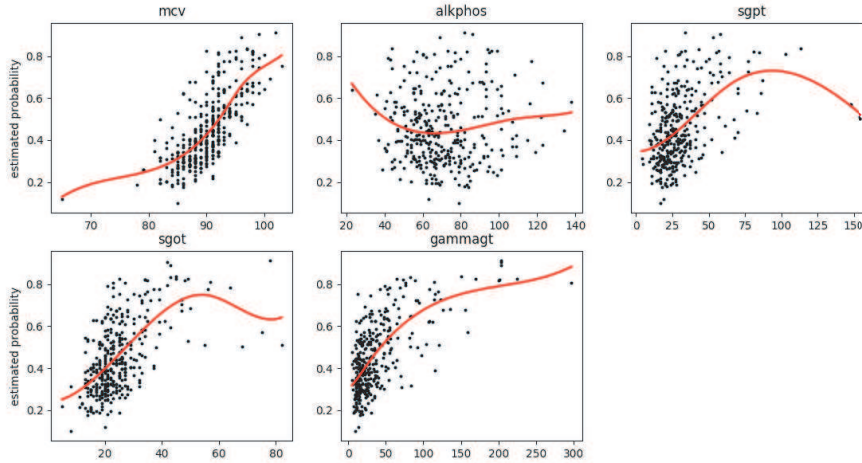


Figure 8: The estimated conditional probabilities from SDRN versus mcv, alkphos, sgot and gammagt for the BUPA data.

the regression function belongs to the Korobov spaces with mixed partial derivatives.

We derive non-asymptotic excess risk bounds for the SDRN estimator. Our framework allows the dimension of the feature space to increase with the sample size at a rate slightly slower than  $\log(n)$ . We further show that our SDRN estimator can achieve the same optimal minimax rate (up to logarithmic factors) as one-dimensional nonparametric regression when the dimension is fixed, and the dimensionality effect is passed on to a logarithmic factor, so the curse of dimensionality is alleviated. The SDRN estimator has a slightly slower rate when the dimension increases with the sample size. Moreover, the depth and the total number of nodes and weights of the network need to increase with the sample size with certain rates established in the paper. These statistical properties provide an important theoretical basis and guidance for the analytic procedures in data analysis. Practically, we illustrate the proposed method through simulation studies and several real data applications. The numerical studies support our theoretical results.

Our proposed method provides a reliable solution for mitigating the curse of dimensionality for modern data analysis. Meanwhile, it has opened up several interesting new avenues for further work. One extension is to derive a similar estimator for smoother regression functions with mixed derivatives of order greater than two; Jacobi-weighted

Korobov spaces (J. Shen & Wang, 2010; Li, Tang, & Yu, 2020) may be considered for this scenario. Our method can be extended to other settings such as semiparametric models, longitudinal data and  $L_1$  penalized regression. Moreover, it can be a promising tool for the estimation of the propensity score function or the outcome regression function used in treatment effect studies. These interesting topics deserve thorough investigations for future research.

## Acknowledgments

We thank the editor and the anonymous reviewer for their valuable comments and suggestions for greatly improving the manuscript. This research was supported in part by the U.S. NSF grants DMS-17-12558, DMS-20-14221 and DMS-23-10288 and the UCR Academic Senate CoR Grant.

## Appendix

In the Appendix, we provide the discussions of sparse grids approximation and the technical proofs.

### A.1 Sparse grids approximation

In this section, we introduce a hierarchical basis of piecewise linear functions. We have discussed a connection between this hierarchical basis and a ReLU network in Section 3. For any functions in the Korobov spaces satisfying Assumption 1, they have a unique representation in this hierarchical basis. To approximate functions of one variable  $x$  on  $[0, 1]$ , a simple choice of a basis function is the standard hat function  $\phi(x)$ :

$$\phi(x) = \begin{cases} 1 - |x|, & \text{if } x \in [-1, 1] \\ 0, & \text{otherwise.} \end{cases}$$

To generate a one-dimensional hierarchical basis, we consider a family of grids  $\Omega_\ell$  of level  $\ell$  characterized by a grid size  $h_\ell = 2^{-\ell}$  and  $2^\ell + 1$  points  $x_{\ell,s} = sh_\ell$  for  $0 \leq s \leq 2^\ell$ . On each  $\Omega_\ell$ , the piecewise linear basis functions  $\phi_{\ell,s}$  are given as

$$\phi_{\ell,s}(x) = \phi\left(\frac{x - x_{\ell,s}}{h_\ell}\right), 0 \leq s \leq 2^\ell,$$

on the support  $[x_{\ell,s} - h_\ell, x_{\ell,s} + h_\ell] \cap [0, 1]$ . Note that  $\|\phi_{\ell,s}\|_\infty \leq 1$  for all  $\ell$  and  $s$ . The hierarchical increment spaces  $W_\ell$  on each  $\Omega_\ell$  are given by

$$W_\ell = \text{span}\{\phi_{\ell,s} : s \in I_\ell\},$$

where  $I_\ell = \{s \in \mathbb{N} : 0 \leq s \leq 2^\ell; s \text{ are odd numbers for } \ell \geq 1\}$ . We can see that for each  $\ell \geq 1$ , the supports of all basis functions  $\phi_{\ell,s}$  spanning  $W_\ell$  are mutually disjoint. Then the hierarchical space of functions up to level  $L$  is

$$V_L = \bigoplus_{0 \leq \ell \leq L} W_\ell = \text{span}\{\phi_{\ell,s} : s \in I_\ell, 0 \leq \ell \leq L\}.$$

To approximate functions of  $d$ -dimensional variables  $\mathbf{x} = (x_1, \dots, x_d)^\top$  on  $\mathcal{X} = [0, 1]^d$ , we employ a tensor product construction of the basis functions. We consider a family of grids  $\Omega_\ell$  of level  $\ell = (\ell_1, \dots, \ell_d)^\top$  with interior points  $\mathbf{x}_{\ell,s} = \mathbf{s} \cdot \mathbf{h}_\ell$ , where  $\mathbf{h}_\ell = (h_{\ell_1}, \dots, h_{\ell_d})^\top$  with  $h_{\ell_j} = 2^{-\ell_j}$  and  $\mathbf{s} = (s_1, \dots, s_d)^\top$  for  $0 \leq s_j \leq 2^{\ell_j}$  and  $j = 1, \dots, d$ . On each  $\Omega_\ell$ , the basis functions  $\phi_{\ell,s}$  are given as

$$\phi_{\ell,s}(\mathbf{x}) = \prod_{j=1}^d \phi_{\ell_j, s_j}(x_j), \mathbf{0}_d \leq \mathbf{s} \leq \mathbf{2}^\ell,$$

and they satisfy  $\|\phi_{\ell,s}\|_\infty \leq 1$ . The hierarchical increment spaces  $W_\ell$  are given by

$$W_\ell = \text{span}\{\phi_{\ell,s}(\mathbf{x}) : \mathbf{s} \in I_\ell\},$$

where  $I_\ell = I_{\ell_1} \times \cdots \times I_{\ell_d}$ , and  $I_{\ell_j} = \{s_j \in \mathbb{N} : 0 \leq s_j \leq 2^{\ell_j}, s_j \text{ are odd numbers for } \ell_j \geq 1\}$ . Then the hierarchical space of functions up to level  $\mathbf{L} = (L_1, \dots, L_d)^\top$  is

$$V_{\mathbf{L}} = \bigoplus_{\mathbf{0} \leq \ell \leq \mathbf{L}} W_\ell = \text{span}\{\phi_{\ell, \mathbf{s}} : \mathbf{s} \in I_\ell, \mathbf{0}_d \leq \ell \leq \mathbf{L}\}.$$

For any function  $f \in W^{2,p}(\mathcal{X})$ , it has a unique expression in the hierarchical basis (Bungartz & Griebel, 2004):

$$f(\mathbf{x}) = \sum_{\mathbf{0}_d \leq \ell \leq \infty} \sum_{\mathbf{s} \in I_\ell} \gamma_{\ell, \mathbf{s}}^0 \phi_{\ell, \mathbf{s}}(\mathbf{x}) = \sum_{\mathbf{0}_d \leq \ell \leq \infty} g_\ell(\mathbf{x}), \quad (\text{A.1})$$

where  $g_\ell(\mathbf{x}) = \sum_{\mathbf{s} \in I_\ell} \gamma_{\ell, \mathbf{s}}^0 \phi_{\ell, \mathbf{s}}(\mathbf{x}) \in W_\ell$ . The hierarchical coefficients  $\gamma_{\ell, \mathbf{s}}^0 \in \mathbb{R}$  are given as (Lemma 3.2 of (Bungartz & Griebel, 2004)):

$$\gamma_{\ell, \mathbf{s}}^0 = \int_{\mathcal{X}} \prod_{j=1}^d (-2^{-(\ell_j+1)} \phi_{\ell_j, s_j}(x_j)) D^{\mathbf{2}} f(\mathbf{x}) d\mathbf{x}, \quad (\text{A.2})$$

where  $\mathbf{2} = 2\mathbf{1}_d$ , and satisfy (Lemma 3.3 of (Bungartz & Griebel, 2004))

$$|\gamma_{\ell, \mathbf{s}}^0| \leq 6^{-d/2} 2^{-(3/2)|\ell|_1} \left( \int_{\mathbf{x}_{\ell, \mathbf{s}} - \mathbf{h}_\ell}^{\mathbf{x}_{\ell, \mathbf{s}} + \mathbf{h}_\ell} |D^{\mathbf{2}} f(\mathbf{x})|^2 d\mathbf{x} \right)^{1/2} \leq 6^{-d/2} 2^{-(3/2)|\ell|_1} \|D^{\mathbf{2}} f\|_{L^2}. \quad (\text{A.3})$$

Moreover, the above result leads to (Lemma 3.4 of (Bungartz & Griebel, 2004))

$$\|g_\ell\|_{L^2} \leq 3^{-d} 2^{-2|\ell|_1} \left( \int_{\mathcal{X}} |D^{\mathbf{2}} f(\mathbf{x})|^2 d\mathbf{x} \right)^{1/2} = 3^{-d} 2^{-2|\ell|_1} \|D^{\mathbf{2}} f\|_{L^2}. \quad (\text{A.4})$$

Assumption 3 and (A.4) imply that

$$\|g_\ell\|_2 \leq c_\mu \|g_\ell\|_{L^2} \leq c_\mu 3^{-d} 2^{-2|\ell|_1} \|D^{\mathbf{2}} f\|_{L^2}. \quad (\text{A.5})$$

In practice, one can use a truncated version to approximate the function  $f(\cdot)$  given



in (A.1), so that

$$f(\mathbf{x}) \approx \sum_{0 \leq |\ell|_\infty \leq m} \sum_{s \in I_\ell} \gamma_{\ell,s}^0 \phi_{\ell,s}(\mathbf{x}) = \sum_{0 \leq |\ell|_\infty \leq m} g_\ell(\mathbf{x}),$$

which is constructed based on the space with full grids:  $V_m^{(\infty)} = \bigoplus_{0 \leq |\ell|_\infty \leq m} W_\ell = \text{span}\{\phi_{\ell,s} : s \in I_\ell, 0 \leq |\ell|_\infty \leq m\}$ . The dimension of the space  $V_m^{(\infty)}$  is  $|V_m^{(\infty)}| = (2^m + 1)^d$ , which increases with  $d$  in an exponential order. For dimension reduction, we consider the hierarchical space with sparse grids:

$$V_m^{(1)} = \bigoplus_{|\ell|_1 \leq m} W_\ell = \text{span}\{\phi_{\ell,s} : s \in I_\ell, |\ell|_1 \leq m\}.$$

The function  $f(\cdot)$  given in (A.1) can be approximated by

$$f_m(\mathbf{x}) = \sum_{|\ell|_1 \leq m} \sum_{s \in I_\ell} \gamma_{\ell,s}^0 \phi_{\ell,s}(\mathbf{x}) = \sum_{|\ell|_1 \leq m} g_\ell(\mathbf{x}). \quad (\text{A.6})$$

Clearly, when  $d = 1$ , the dimension of the hierarchical space with sparse grids is the same as that of the space with full grids. The dimensionality issue does not exist. For the rest of this paper, we assume that  $d \geq 2$ . Table A.1 provides the number of basis functions for the hierarchical space with sparse grids  $V_m^{(1)}$  and the space with full grids  $V_m^{(\infty)}$  when the dimension of the covariates  $d$  increases from 2 to 8 and the  $m$  value increases from 0 to 4. We see that the number of basis functions for the space with sparse grids is dramatically reduced compared to the space with full grids, when the dimension  $d$  or  $m$  value become larger, so that the dimensionality problem can be lessened.

The following proposition provides the approximation error of the approximator  $f_m(\cdot)$  obtained from the sparse grids to the true unknown function  $f \in W^{2,p}(\mathcal{X})$ .

**Proposition A.1.** *For any  $f \in W^{2,p}(\mathcal{X})$ ,  $2 \leq p \leq \infty$ , under Assumption 3, one has*

Table A.1: The number of basis functions for the space with sparse grids and the space with full grids.

	Sparse grids					Full grids				
	$m = 0$	$m = 1$	$m = 2$	$m = 3$	$m = 4$	$m = 0$	$m = 1$	$m = 2$	$m = 3$	$m = 4$
$d = 2$	4	8	17	37	81	4	9	25	81	289
$d = 3$	8	20	50	123	297	8	27	125	729	4913
$d = 4$	16	48	136	368	961	16	81	625	6561	83521
$d = 5$	32	112	352	1032	2882	32	243	3125	59049	1419857
$d = 6$	64	256	880	2768	8204	64	729	15625	531441	24137569
$d = 7$	128	576	2144	7184	22472	128	2187	78125	4782969	410338673
$d = 8$	256	1280	5120	18176	59744	256	6561	390625	43046721	6975757441

that

$$\|f_m - f\|_2 \leq 4^{-1} c_\mu 2^{-2m} (3/2)^{-d} (m+3)^{d-1} \|D^2 f\|_{L^2}. \quad (\text{A.7})$$

Proposition A.1 shows that the approximator error decreases as the  $m$  value increases.

In the following proposition, we provide an upper and a lower bounds for the dimension (cardinality) of the space  $V_m^{(1)}$ .

**Proposition A.2.** *The dimension of the space  $V_m^{(1)}$  satisfies that for  $d \geq 2$ ,*

$$\begin{aligned} 2^{d-1}(2^m + 1) &\leq |V_m^{(1)}| \leq 4 \frac{d}{(d-1)!} 2^d 2^m (m+d)^{d-1} \\ &\leq 4 \sqrt{\frac{2}{\pi}} \frac{d}{\sqrt{d-1}} 2^m \left( 2e \frac{m+d}{d-1} \right)^{d-1}. \end{aligned}$$

**Remark 13.** (Bungartz & Griebel, 2004) gives an asymptotic order for the cardinality of  $V_m^{(1)}$  which is  $|V_m^{(1)}| = \mathcal{O}(c(d)2^m m^{d-1})$ , where  $c(d)$  is a constant depending on  $d$ , and the form of  $c(d)$  has not been provided. (Montanelli & Du, 2019) numerically demonstrated how quickly  $c(d)$  can increase with  $d$ . In Proposion A.2, we give an explicit form for the upper bound of  $|V_m^{(1)}|$  that has not been derived in the literature. From this explicit form, we can more clearly see how the dimension of  $V_m^{(1)}$  increases with  $d$ .

## A.2 Proof of Proposition A.1

This section provides the proof of Proposition A.1. Based on (A.1) and (A.6), one has

$$\|f_m - f\|_2 = \left\| \sum_{\mathbf{0}_d \leq \boldsymbol{\ell} \leq \infty} g_{\boldsymbol{\ell}}(\mathbf{x}) - \sum_{|\boldsymbol{\ell}_1| \leq m} g_{\boldsymbol{\ell}}(\mathbf{x}) \right\|_2 = \left\| \sum_{|\boldsymbol{\ell}_1| > m} g_{\boldsymbol{\ell}}(\mathbf{x}) \right\|_2.$$

By (A.5) and Assumption 3, one has

$$\begin{aligned} \left\| \sum_{|\boldsymbol{\ell}_1| > m} g_{\boldsymbol{\ell}}(\mathbf{x}) \right\|_2 &\leq \sum_{|\boldsymbol{\ell}_1| > m} \|g_{\boldsymbol{\ell}}\|_2 \leq \sum_{|\boldsymbol{\ell}_1| > m} c_{\mu} 3^{-d} 2^{-2|\boldsymbol{\ell}_1|} \|D^{\mathbf{2}} f\|_{L^2} \\ &= c_{\mu} 3^{-d} \|D^{\mathbf{2}} f\|_{L^2} \sum_{|\boldsymbol{\ell}_1| > m} 2^{-2|\boldsymbol{\ell}_1|}. \end{aligned}$$

Then, one has that for arbitrary  $s \in \mathbb{N}$ ,

$$\begin{aligned} \sum_{|\boldsymbol{\ell}_1| > m} 2^{-s|\boldsymbol{\ell}_1|} &= \sum_{k'=m+1}^{\infty} 2^{-sk'} \binom{k' + d - 1}{d - 1} \\ &= \sum_{k=0}^{\infty} 2^{-s(k+m+1)} \binom{k + m + 1 + d - 1}{d - 1} \\ &= 2^{-s(m+1)} \sum_{k=0}^{\infty} 2^{-sk} \binom{k + m + 1 + d - 1}{d - 1} \\ &\leq 2^{-s(m+1)} 2A(d, m), \end{aligned}$$

where  $A(d, m) = \sum_{k=0}^{d-1} \binom{m+d}{k}$ , where the last inequality follows from Lemma 3.7 of (Bungartz & Griebel, 2004).

$$\begin{aligned} \|f_m - f\|_2 &\leq \sum_{|\boldsymbol{\ell}_1| > m} \|g_{\boldsymbol{\ell}}\|_2 \leq c_{\mu} 3^{-d} \|D^{\mathbf{2}} f\|_{L^2} 2^{-2(m+1)} 2A(d, m) \\ &= 2^{-1} c_{\mu} 2^{-2m} 3^{-d} A(d, m) \|D^{\mathbf{2}} f\|_{L^2}. \end{aligned}$$

Moreover,

$$\begin{aligned} A(d, m) &= \sum_{k=0}^{d-1} \binom{d-1}{k} \frac{(m+d)!(d-1-k)!}{(m+d-k)!(d-1)!} \\ &= \sum_{k=0}^{d-1} \binom{d-1}{k} \left( \frac{m+d}{d-1} \right) \left( \frac{m+d-1}{d-2} \right) \cdots \left( \frac{m+d-k+1}{d-k} \right). \end{aligned}$$

Since  $\left( \frac{m+d-j+1}{d-j} \right) > \left( \frac{m+d-j'+1}{d-j'} \right)$  for any  $1 \leq j' < j \leq d-1$ , then  $\left( \frac{m+2}{1} \right) > \left( \frac{m+d-j'+1}{d-j'} \right)$  for any  $1 \leq j' \leq d-1$  by letting  $j = d-1$ , and thus

$$A(d, m) \leq \sum_{k=0}^{d-1} \binom{d-1}{k} (m+2)^k = (m+3)^{d-1}.$$

Therefore,

$$\begin{aligned} \|f_m - f\|_2 &\leq 2^{-1} c_\mu 2^{-2m} 3^{-d} 2^{d-1} (m+3)^{d-1} \|D^2 f\|_{L^2} \\ &= 4^{-1} c_\mu 2^{-2m} (3/2)^{-d} (m+3)^{d-1} \|D^2 f\|_{L^2}. \end{aligned}$$

### A.3 Proof of Proposition A.2

In this section, we provide the proof of Proposition A.2. The dimension of  $W_\ell$  satisfies

$$|W_\ell| \leq \prod_{j=1}^d 2^{\ell_j \vee 2-1} = 2^{\sum_{j=1}^d \ell_j \vee 2-d}.$$

Thus,

$$\begin{aligned} |V_m^{(1)}| &\leq \sum_{|\ell|_1 \leq m} 2^{\sum_{j=1}^d \ell_j \vee 2-d} \leq \sum_{|\ell|_1 \leq m} 2^{|\ell|_1+d} = \sum_{k=0}^m 2^{k+d} \binom{d-1+k}{d-1} \\ &= 2^d \sum_{k=0}^m 2^k \binom{d-1+k}{d-1} = 2^d \left\{ (-1)^d + 2^{m+1} \sum_{k=0}^{d-1} \binom{m+d}{k} (-2)^{d-1-k} \right\}, \end{aligned}$$

where the last equality follows from (3.62) of (Bungartz & Griebel, 2004). We assume that  $d$  is even. The result for odd  $d$  can be proved similarly. Then

$$\sum_{k=0}^{d-1} \binom{m+d}{k} (-2)^{d-1-k} = \sum_{v=0}^{d/2-1} 2^{2v} \left\{ \binom{m+d}{d-(1+2v)} - 2 \binom{m+d}{d-(2+2v)} \right\}.$$

Moreover,

$$\begin{aligned} & \binom{m+d}{d-(1+2v)} - 2 \binom{m+d}{d-(2+2v)} \\ &= \frac{(m+d)!}{(d-(1+2v))!(m+1+2v)!} - 2 \frac{(m+d)!}{(d-(2+2v))!(m+2v+2)!} \\ &= \frac{(m+d)!}{(d-(2+2v))!(m+1+2v)!} \left\{ \frac{1}{d-(1+2v)} - \frac{2}{m+2v+2} \right\} \\ &= \frac{(m+d)!(m+6v-2d+4)}{(d-(1+2v))!(m+2v+2)!} \\ &= \frac{(m+d)(m+d-1) \times \cdots \times (m+2v+3)(m+6v-2d+4)}{(d-(1+2v))!} \\ &\leq \frac{(m+d)^{d-(1+2v)}}{(d-(1+2v))!}. \end{aligned}$$

Thus,

$$\begin{aligned} \sum_{k=0}^{d-1} \binom{m+d}{k} (-2)^{d-1-k} &\leq \sum_{v=0}^{d/2-1} 2^{2v} \frac{(m+d)^{d-(1+2v)}}{(d-(1+2v))!} \\ &\leq \frac{(m+d)^{(d-1)}}{(d-1)!} \sum_{v=0}^{d/2-1} \frac{2^{2v}}{(m+d)^{2v}} \\ &\leq \frac{(m+d)^{(d-1)}}{(d-1)!} \frac{m+d}{m+d-2} \leq \frac{(m+d)^{d-1}}{(d-1)!} d, \end{aligned}$$

for  $m+d \geq 3$  and  $d \geq 3$ . It is easy to verify that  $\sum_{k=0}^{d-1} \binom{m+d}{k} (-2)^{d-1-k} \leq (m+d)^{(d-1)} d / (d-1)!$

when  $d \leq 2$  or  $m+d \leq 2$ .

By stirling's formula,

$$(d-1)! \geq \sqrt{2\pi} (d-1)^{d-1/2} e^{-(d-1)}.$$

Therefore, for  $d \geq 2$ ,

$$\sum_{k=0}^{d-1} \binom{m+d}{k} (-2)^{d-1-k} \leq \frac{(m+d)^{d-1}}{(d-1)!} d \leq \frac{(m+d)^{d-1} d}{\sqrt{2\pi}(d-1)^{d-1/2} e^{-(d-1)}},$$

and hence

$$\begin{aligned} |V_m^{(1)}| &\leq 2^{d+1} 2^{m+1} \frac{(m+d)^{d-1}}{(d-1)!} d \leq 2^{d+1} 2^{m+1} \frac{(m+d)^{d-1} d}{\sqrt{2\pi}(d-1)^{d-1/2} e^{-(d-1)}} \\ &= 4 \sqrt{\frac{2}{\pi}} \frac{d}{\sqrt{d-1}} 2^m \left( 2e \frac{m+d}{d-1} \right)^{d-1}. \end{aligned}$$

Moreover, let  $\ell_{-1} = (\ell_2, \dots, \ell_d)^\top$ . Then,  $|V_0^{(1)}| = \sum_{|\ell_1|=0} \prod_{j=1}^d 2 = 2^d$ , and for  $m \geq 1$ ,

$$\begin{aligned} |V_m^{(1)}| &\geq \sum_{|\ell_1|=0} \prod_{j=1}^d 2 + \sum_{1 \leq \ell_1 \leq m, |\ell_{-1}|_1=0} \left( \prod_{j=2}^d 2 \right) 2^{\ell_1-1} \\ &= 2^d + 2^{d-1} \sum_{1 \leq \ell_1 \leq m} 2^{\ell_1-1} = 2^d + 2^{d-1} (2^m - 1) \\ &= 2^{d-1} (2^m - 1 + 2) \geq 2^{d-1} (2^m + 1). \end{aligned}$$

Therefore,  $|V_m^{(1)}| \geq 2^{d-1} (2^m + 1)$  for any  $m \geq 0$ .

#### A.4 Proof of Proposition 1

In this section, we provide the proof of Proposition 1. It is clear that  $\|\tilde{f} - f\|_2 = \|\tilde{f} - f_m + f_m - f\|_2 \leq \|\tilde{f} - f_m\|_2 + \|f_m - f\|_2$ . The rate of  $\|f_m - f\|_2$  is provided in Proposition A.1. Next we derive the rate of  $\|\tilde{f} - f_m\|_2$  as follows. By (A.6) and (6), we have

$$\|\tilde{f} - f_m\|_2 \leq \sup_{\mathbf{x} \in \mathcal{X}} \sum_{|\ell_1| \leq m} \sum_{s \in I_\ell} |\gamma_{\ell,s}^0| |\tilde{\varphi}_R(\phi_{\ell,s}(\mathbf{x})) - \phi_{\ell,s}(\mathbf{x})|.$$

Since a given  $\boldsymbol{x}$  belongs to at most one of the disjoint supports for  $\phi_{\boldsymbol{\ell}, \boldsymbol{s}_{\boldsymbol{\ell}}}(\boldsymbol{x})$ , this result together with (5) lead to

$$\|\tilde{f} - f_m\|_2 \leq 3 \cdot 2^{-2R-2}(d-1) \sum_{|\boldsymbol{\ell}|_1 \leq m} |\gamma_{\boldsymbol{\ell}, \boldsymbol{s}_{\boldsymbol{\ell}}}^0|,$$

for some  $\boldsymbol{s}_{\boldsymbol{\ell}}$ . Moreover, by (A.3), we have

$$\begin{aligned} \sum_{|\boldsymbol{\ell}|_1 \leq m} |\gamma_{\boldsymbol{\ell}, \boldsymbol{s}_{\boldsymbol{\ell}}}^0| &\leq \sum_{|\boldsymbol{\ell}|_1 \leq m} 6^{-d/2} 2^{-(3/2)|\boldsymbol{\ell}|_1} \|D^{\mathbf{2}} f\|_{L^2} \\ &= 6^{-d/2} \|D^{\mathbf{2}} f\|_{L^2} \sum_{|\boldsymbol{\ell}|_1 \leq m} 2^{-(3/2)|\boldsymbol{\ell}|_1} \\ &= 6^{-d/2} \|D^{\mathbf{2}} f\|_{L^2} \sum_{k=0}^m 2^{-(3/2)k} \binom{k+d-1}{d-1}. \end{aligned}$$

Since  $\sum_{k=0}^{\infty} \left(\frac{1}{\sqrt{8}}\right)^k \left(1 - \frac{1}{\sqrt{8}}\right)^d \binom{k+d-1}{d-1} = 1$ , it implies that

$$\sum_{k=0}^m 2^{-(3/2)k} \binom{k+d-1}{d-1} \leq \sum_{k=0}^{\infty} 2^{-(3/2)k} \binom{k+d-1}{d-1} = \left(1 - \frac{1}{\sqrt{8}}\right)^{-d},$$

and thus

$$\sum_{|\boldsymbol{\ell}|_1 \leq m} |\gamma_{\boldsymbol{\ell}, \boldsymbol{s}_{\boldsymbol{\ell}}}^0| \leq \left\{ \sqrt{6} \left(1 - \frac{1}{\sqrt{8}}\right) \right\}^{-d} \|D^{\mathbf{2}} f\|_{L^2} \leq (\sqrt{3/2})^{-d} \|D^{\mathbf{2}} f\|_{L^2}. \quad (\text{A.8})$$

Therefore,

$$\begin{aligned} \|\tilde{f} - f_m\|_2 &\leq 3 \cdot 2^{-2R-2}(d-1)(\sqrt{3/2})^{-d} \|D^{\mathbf{2}} f\|_{L^2} \\ &= (3/4)2^{-2R}(d-1)(\sqrt{3/2})^{-d} \|D^{\mathbf{2}} f\|_{L^2}. \end{aligned}$$

The above result and (A.7) lead to

$$\begin{aligned}
\|\tilde{f} - f\|_2 &\leq \|\tilde{f} - f_m\|_2 + \|f_m - f\|_2 \\
&\leq \left\{ (3/4)2^{-2R}(d-1)(\sqrt{3/2})^{-d} + 4^{-1}c_\mu 2^{-2m}(3/2)^{-d}(m+3)^{d-1} \right\} \|D^2 f\|_{L^2} \\
&\leq \left\{ (3/2)2^{-2R} + 4^{-1}c_\mu 2^{-2m}(3/2)^{-d}(m+3)^{d-1} \right\} \|D^2 f\|_{L^2} \\
&= \left\{ (3/2)2^{-2R} + 6^{-1}c_\mu 2^{-2m} \{(2/3)(m+3)\}^{d-1} \right\} \|D^2 f\|_{L^2}.
\end{aligned}$$

Moreover, the ReLU network used to construct the approximator  $\tilde{f}$  has depth  $\mathcal{O}(R \log_2 d)$ , the number of weights  $\mathcal{O}(Rd) \times |V_m^{(1)}|$ , and the computational units  $\mathcal{O}(Rd) \times |V_m^{(1)}|$ . By the upper bound for  $|V_m^{(1)}|$  established in Proposition (A.2), we have that the number of weights is  $\mathcal{O}\left(2^m d^{3/2} R \left(2e \frac{m+d}{d-1}\right)^{d-1}\right)$ , and the number of the computational units is  $\mathcal{O}(Rd) \times \mathcal{O}\left(2^m \frac{d}{\sqrt{d-1}} \left(2e \frac{m+d}{d-1}\right)^{d-1}\right) = \mathcal{O}\left(2^m d^{3/2} R \left(2e \frac{m+d}{d-1}\right)^{d-1}\right)$ .

## A.5 Proofs of Proposition 2

Under Condition (11) given in Assumption 5, by the definition of  $f^*$  given in (9) and Proposition 1, the approximation error satisfies that for  $d \geq 2$  and  $R \geq m$ ,

$$\begin{aligned}
\mathcal{E}(f^*) - \mathcal{E}(f_0) &\leq \mathcal{E}(\tilde{f}) - \mathcal{E}(f_0) \leq b_\rho \|\tilde{f} - f_0\|_2^2 \\
&\leq b_\rho \left\{ (3/2)2^{-2R} + 6^{-1}c_\mu 2^{-2m} \{(2/3)(m+3)\}^{d-1} \right\}^2 \|D^2 f_0\|_{L^2}^2 \\
&\leq b_\rho \left\{ (3/2)2^{-2m} + 6^{-1}c_\mu 2^{-2m} \{(2/3)(m+3)\}^{d-1} \right\}^2 \|D^2 f_0\|_{L^2}^2 \\
&\leq \zeta_{m,d},
\end{aligned}$$

where

$$\zeta_{m,d} = 4^{-1}b_\rho(3 + c_\mu/3)^2 2^{-4m} \{(2/3)(m+3)\}^{2(d-1)} \|D^2 f_0\|_{L^2}^2.$$

## A.6 Proofs of theorems 1 and 2

We first introduce a Bernstein inequality which will be used to establish the bounds in Theorems 1 and 2.



**Lemma A.1.** Let  $\mathcal{G}$  be a set of scalar-valued functions on  $\mathcal{X} \times \mathcal{Y}$  such that for each  $\xi(\mathbf{X}, Y) \in \mathcal{G}$ ,  $\mathbb{E}\{\xi(\mathbf{X}, Y)\} \geq 0$ ,  $\mathbb{E}\{\xi(\mathbf{X}, Y)^2\} \leq c_1 \mathbb{E}\{\xi(\mathbf{X}, Y)\}$  and  $|\xi(\mathbf{X}, Y) - \mathbb{E}\{\xi(\mathbf{X}, Y)\}| \leq c_2$  almost everywhere for some constants  $c_1, c_2 \in (0, \infty)$ . Then for every  $\epsilon > 0$  and  $0 < \alpha \leq 1$ , we have

$$\begin{aligned} & P \left\{ \sup_{\xi \in \mathcal{G}} \frac{\mathbb{E}\{\xi(\mathbf{X}, Y)\} - n^{-1} \sum_{i=1}^n \xi(\mathbf{X}_i, Y_i)}{\sqrt{\mathbb{E}\{\xi(\mathbf{X}, Y)\} + \epsilon}} > 4\alpha\sqrt{\epsilon} \right\} \\ & \leq \mathcal{N}(\alpha\epsilon, \mathcal{G}, \|\cdot\|_\infty) \exp\left(-\frac{\alpha^2 n \epsilon}{2c_1 + 2c_2/3}\right). \end{aligned}$$

*Proof.* Let  $\{\xi_j\}_{j=1}^J \in \mathcal{G}$  with  $J = \mathcal{N}(\alpha\epsilon, \mathcal{G}, \|\cdot\|_\infty)$  being such that  $\mathcal{G}$  is covered by  $\|\cdot\|_\infty$ -balls centered on  $\xi_j$  with radius  $\alpha\epsilon$ . Denote  $\mu(\xi) = \mathbb{E}\{\xi(\mathbf{X}, Y)\}$  and  $\sigma^2(\xi) = \text{var}\{\xi(\mathbf{X}, Y)\}$ . For each  $j$ , by applying the one-side Bernstein inequality in Corollary 3.6 of (Cucker & Zhou, 2007), one has

$$\begin{aligned} & P \left\{ \frac{\mu(\xi_j) - n^{-1} \sum_{i=1}^n \xi_j(\mathbf{X}_i, Y_i)}{\sqrt{\mu(\xi_j) + \epsilon}} > \alpha\sqrt{\epsilon} \right\} \\ & \leq \exp\left(-\frac{\alpha^2 n (\mu(\xi_j) + \epsilon) \epsilon}{2\{\sigma^2(\xi_j) + c_2 \alpha \sqrt{\mu(\xi_j) + \epsilon} \sqrt{\epsilon}/3\}}\right). \end{aligned} \quad (\text{A.9})$$

Since  $\sigma^2(\xi_j) \leq \mathbb{E}\{\xi_j(\mathbf{X}, Y)^2\} \leq c_1 \mu(\xi_j)$ , then

$$\begin{aligned} & \sigma^2(\xi_j) + c_2 \alpha \sqrt{\mu(\xi_j) + \epsilon} \sqrt{\epsilon}/3 \\ & \leq c_1 \mu(\xi_j) + c_2 (\mu(\xi_j) + \epsilon)/3 \\ & \leq c_1 (\mu(\xi_j) + \epsilon) + c_2 (\mu(\xi_j) + \epsilon)/3 \\ & = (c_1 + c_2/3) (\mu(\xi_j) + \epsilon). \end{aligned}$$

The above result together with (A.9) implies that

$$\begin{aligned} & P \left\{ \frac{\mu(\xi_j) - n^{-1} \sum_{i=1}^n \xi_j(\mathbf{X}_i, Y_i)}{\sqrt{\mu(\xi_j) + \epsilon}} > \alpha\sqrt{\epsilon} \right\} \\ & \leq \exp \left( -\frac{\alpha^2 n (\mu(\xi_j) + \epsilon) \epsilon}{2(c_1 + c_2/3)(\mu(\xi_j) + \epsilon)} \right) = \exp \left( -\frac{\alpha^2 n \epsilon}{2(c_1 + c_2/3)} \right). \end{aligned} \quad (\text{A.10})$$

For each  $\xi \in \mathcal{G}$ , there exists some  $j$  such that  $\|\xi - \xi_j\|_\infty \leq \alpha\epsilon$ . Then  $|\mu(\xi) - \mu(\xi_j)|$  and  $|n^{-1} \sum_{i=1}^n \xi(\mathbf{X}_i, Y_i) - n^{-1} \sum_{i=1}^n \xi_j(\mathbf{X}_i, Y_i)|$  are both bounded by  $\alpha\epsilon$ . Hence,

$$\frac{|\mu(\xi) - \mu(\xi_j)|}{\sqrt{\mu(\xi) + \epsilon}} \leq \alpha\sqrt{\epsilon}, \quad \frac{|n^{-1} \sum_{i=1}^n \xi(\mathbf{X}_i, Y_i) - n^{-1} \sum_{i=1}^n \xi_j(\mathbf{X}_i, Y_i)|}{\sqrt{\mu(\xi) + \epsilon}} \leq \alpha\sqrt{\epsilon}.$$

This implies that

$$\begin{aligned} \mu(\xi_j) + \epsilon &= \mu(\xi_j) - \mu(\xi) + \mu(\xi) + \epsilon \\ &\leq \alpha\sqrt{\epsilon} \sqrt{\mu(\xi) + \epsilon} + \{\mu(\xi) + \epsilon\} \\ &\leq \sqrt{\epsilon} \sqrt{\mu(\xi) + \epsilon} + \{\mu(\xi) + \epsilon\} \\ &\leq 2\{\mu(\xi) + \epsilon\}, \end{aligned}$$

so that  $\sqrt{\mu(\xi_j) + \epsilon} \leq 2\sqrt{\{\mu(\xi) + \epsilon\}}$ . Therefore,  $\{\mu(\xi) - n^{-1} \sum_{i=1}^n \xi(\mathbf{X}_i, Y_i)\} / \sqrt{\mu(\xi) + \epsilon} \geq 4\alpha\sqrt{\epsilon}$  implies that  $\{\mu(\xi_j) - n^{-1} \sum_{i=1}^n \xi_j(\mathbf{X}_i, Y_i)\} / \sqrt{\mu(\xi) + \epsilon} \geq 2\alpha\sqrt{\epsilon}$  and thus  $\{\mu(\xi_j) - n^{-1} \sum_{i=1}^n \xi_j(\mathbf{X}_i, Y_i)\} / \sqrt{\mu(\xi_j) + \epsilon} \geq \alpha\sqrt{\epsilon}$ . This result together with (A.10) implies

$$\begin{aligned} & P \left\{ \sup_{\xi \in \mathcal{G}} \frac{\mu(\xi) - n^{-1} \sum_{i=1}^n \xi(\mathbf{X}_i, Y_i)}{\sqrt{\mu(\xi) + \epsilon}} > 4\alpha\sqrt{\epsilon} \right\} \\ & \leq \sum_{j=1}^J P \left\{ \frac{\mu(\xi_j) - n^{-1} \sum_{i=1}^n \xi_j(\mathbf{X}_i, Y_i)}{\sqrt{\mu(\xi_j) + \epsilon}} > \alpha\sqrt{\epsilon} \right\} \leq J \exp \left( -\frac{\alpha^2 n \epsilon}{2c_1 + 2c_2/3} \right). \end{aligned}$$

□

Based on the Bernstein inequality given in Lemma A.1, we next provide a proba-

bility bound that will be used for establishing an upper bound for the sampling error  $\mathcal{E}(\widehat{f}) - \mathcal{E}(f^*)$ . For notational simplicity, we denote  $\mathcal{E}_n(f; \Theta) := \mathcal{E}_n(f)$ .

**Lemma A.2.** *Under Assumptions 1-4, we have that for any  $\epsilon > 0$  and  $0 < \alpha \leq 1$ ,*

$$P \left\{ \sup_{f \in \mathcal{F}(R, m, B_0, B_1)} \frac{\mathcal{E}(f) - \mathcal{E}(f^*) - (\mathcal{E}_n(f) - \mathcal{E}_n(f^*))}{\sqrt{\mathcal{E}(f) - \mathcal{E}(f^*) + \epsilon}} > 4\alpha\sqrt{\epsilon} \right\} \\ \leq \mathcal{N}(\alpha C_\rho^{-1} \epsilon, \mathcal{F}(R, m, B_0, B_1), \|\cdot\|_\infty) \exp\left(-\frac{\alpha^2 n \epsilon}{2C_\rho^2 a_\rho^{-1} + 8M_\rho/3}\right),$$

where  $C_\rho$ ,  $a_\rho$  and  $M_\rho$  are constants given in Assumptions 2 and 4 and Remark 7.

*Proof.* Let  $\mathcal{G} = \{\xi(\mathbf{x}, y) = \rho(f(\mathbf{x}), y) - \rho(f^*(\mathbf{x}), y); f \in \mathcal{F}(R, m, B_0, B_1), (\mathbf{x}, y) \in \mathcal{X} \times \mathcal{Y}\}$ . For any  $f \in \mathcal{F}(R, m, B_0, B_1)$ ,

$$\mathbb{E}\{\xi(\mathbf{X}, Y)\} = \mathbb{E}\{\rho(f(\mathbf{X}), Y)\} - \mathbb{E}\{\rho(f^*(\mathbf{X}), Y)\} \geq 0,$$

based on the definition of  $f^*$  given in (9). By Remark 7, we have  $|\xi(\mathbf{x}, y)| \leq 2M_\rho$ , for almost every  $(\mathbf{x}, y) \in \mathcal{X} \times \mathcal{Y}$ , so that

$$|\xi(\mathbf{X}, Y) - \mathbb{E}\{\xi(\mathbf{X}, Y)\}| \leq 4M_\rho,$$

almost surely. Moreover, Assumption 2 further implies that  $|\xi(\mathbf{x}, y)| \leq C_\rho |f(\mathbf{x}) - f^*(\mathbf{x})|$  for almost every  $(\mathbf{x}, y) \in \mathcal{X} \times \mathcal{Y}$ . Then

$$\mathbb{E}\{\xi(\mathbf{X}, Y)^2\} \leq C_\rho^2 \int_{\mathcal{X}} |f(\mathbf{x}) - f^*(\mathbf{x})|^2 d\mu_X(\mathbf{x}) = C_\rho^2 \|f - f^*\|_2^2. \quad (\text{A.11})$$

Moreover, under Condition (10) in Assumption 4,

$$\|f - f^*\|_2^2 \leq a_\rho^{-1} \{\mathcal{E}(f) - \mathcal{E}(f^*)\}.$$

Thus

$$\mathbb{E}\{\xi(\mathbf{X}, Y)^2\} \leq a_\rho^{-1} C_\rho^2 \{\mathcal{E}(f) - \mathcal{E}(f^*)\} = a_\rho^{-1} C_\rho^2 \mathbb{E}\{\xi(\mathbf{X}, Y)\}. \quad (\text{A.12})$$

By the Bernstein inequality given in Lemma A.1, for every  $\epsilon > 0$  and  $0 < \alpha \leq 1$ , we have

$$\begin{aligned} & P \left\{ \sup_{f \in \mathcal{F}(R, m, B_0, B_1)} \frac{\mathcal{E}(f) - \mathcal{E}(f^*) - (\mathcal{E}_n(f) - \mathcal{E}_n(f^*))}{\sqrt{\mathcal{E}(f) - \mathcal{E}(f^*) + \epsilon}} > 4\alpha\sqrt{\epsilon} \right\} \\ & \leq \mathcal{N}(\alpha\epsilon, \mathcal{G}, \|\cdot\|_\infty) \exp\left(-\frac{\alpha^2 n \epsilon}{2C_\rho^2 a_\rho^{-1} + 8M_\rho/3}\right). \end{aligned}$$

Since  $|\rho(f(\mathbf{x}), y) - \rho(f^*(\mathbf{x}), y)| \leq C_\rho |f(\mathbf{x}) - f^*(\mathbf{x})|$  for almost every  $(\mathbf{x}, y) \in \mathcal{X} \times \mathcal{Y}$ , it follows that

$$\mathcal{N}(\alpha\epsilon, \mathcal{G}, \|\cdot\|_\infty) \leq \mathcal{N}(\alpha C_\rho^{-1} \epsilon, \mathcal{F}(R, m, B_0, B_1), \|\cdot\|_\infty).$$

□

*Proof of Theorem 1.* Let  $f = \hat{f}$ ,  $\Delta = \mathcal{E}(\hat{f}) - \mathcal{E}(f^*)$  and  $\alpha = \sqrt{2}/8$ . From the result in Lemma A.2, we have

$$P \left\{ \frac{\Delta - (\mathcal{E}_n(\hat{f}) - \mathcal{E}_n(f^*))}{\sqrt{\Delta + \epsilon}} > \sqrt{\epsilon/2} \right\} \leq Q, \quad (\text{A.13})$$

where

$$Q = \mathcal{N}(\sqrt{2}C_\rho^{-1}\epsilon/8, \mathcal{F}(R, m, B_0, B_1), \|\cdot\|_\infty) \exp(-n\epsilon/C^*),$$

in which  $C^* = 64(C_\rho^2 a_\rho^{-1} + 4M_\rho/3)$ . Let  $\Delta_n = (\mathcal{E}_n(\hat{f}) + 2^{-1}\lambda \hat{\Theta}^\top \hat{\Theta} - \mathcal{E}_n(f^*) -$

$2^{-1}\lambda\Theta^{*\top}\Theta^*$ ). We have  $\Delta_n \leq \varpi_n$ ,  $\widehat{\Theta}^\top\widehat{\Theta} \leq B_1^2$  and  $\Theta^{*\top}\Theta^* \leq B_1^2$ . Then

$$\begin{aligned}
\frac{\Delta - (\mathcal{E}_n(\widehat{f}) - \mathcal{E}_n(f^*))}{\sqrt{\Delta + \epsilon}} &= \frac{\Delta + (2^{-1}\lambda\widehat{\Theta}^\top\widehat{\Theta} - 2^{-1}\lambda\Theta^{*\top}\Theta^*) - \Delta_n}{\sqrt{\Delta + \epsilon}} \\
&\geq \frac{\Delta - \varpi_n}{\sqrt{\Delta + \epsilon}} + \frac{2^{-1}\lambda(\widehat{\Theta}^\top\widehat{\Theta} - \Theta^{*\top}\Theta^*)}{\sqrt{\Delta + \epsilon}}. \\
&\geq \frac{\Delta - \varpi_n}{\sqrt{\Delta + \epsilon}} - \frac{2^{-1}\lambda 2B_1^2}{\sqrt{\Delta + \epsilon}} \\
&= \frac{\Delta}{\sqrt{\Delta + \epsilon}} - \frac{(\varpi_n + \lambda B_1^2)}{\sqrt{\Delta + \epsilon}}. \tag{A.14}
\end{aligned}$$

The above result and (A.13) lead to

$$P\left\{\Delta > \sqrt{\epsilon/2}\sqrt{\Delta + \epsilon} + (\varpi_n + \lambda B_1^2)\right\} \leq Q.$$

Moreover,

$$\begin{aligned}
\Delta &> \sqrt{\epsilon/2}\sqrt{\Delta + \epsilon} + \varpi_n + \lambda B_1^2 \\
&\iff (\Delta - (\varpi_n + \lambda B_1^2))^2 > (\epsilon/2)(\Delta + \epsilon) \\
&\iff (\Delta - (\varpi_n + \lambda B_1^2) - \epsilon/4)^2 > (9/16)\epsilon^2 \\
&\iff \Delta - (\varpi_n + \lambda B_1^2) > \epsilon \text{ or } \Delta - (\varpi_n + \lambda B_1^2) < -(1/2)\epsilon.
\end{aligned}$$

Since  $\Delta \geq 0$  and  $\varpi_n + \lambda B_1^2 < (1/2)\epsilon$ , then  $P\left\{\Delta > \sqrt{\epsilon/2}\sqrt{\Delta + \epsilon} + (\varpi_n + \lambda B_1^2)\right\} \leq Q$  is equivalent to  $P(\Delta > \epsilon + \varpi_n + \lambda B_1^2) \leq Q$ . Given that  $\varpi_n + \lambda B_1^2 < (1/2)\epsilon$ , one has  $P(\Delta > (3/2)\epsilon) \leq P(\Delta > \epsilon + \varpi_n + \lambda B_1^2) \leq Q$ .  $\square$

*Proof of Theorem 2.* For the sparse deep ReLU network given in Section 5, the number of parameters is  $W = |V_m^{(1)}| + (12R - 6) + 4 + 3 = |V_m^{(1)}| + 12R + 1 \asymp |V_m^{(1)}| + R$  and the number of layers is  $L \asymp R \log_2 d$ . Let  $d(W, L)$  denote the pseudo-dimension of the ReLU network class  $\mathcal{F}(R, m, B_0, B_1)$  defined in (Bartlett, Harvey, Liaw, & Mehrabian, 2019). By the result given in equation (2) of (Bartlett et al., 2019), one has that there

exist constants  $c, C$  such that

$$c \cdot WL \log(W/L) \leq d(W, L) \leq C \cdot WL \log(W). \quad (\text{A.15})$$

By Theorem 12.2 in (Anthony & Bartlett, 2009), one has

$$\mathcal{N}(\sqrt{2}C_\rho^{-1}\epsilon/8, \mathcal{F}(R, m, B_0, B_1), \|\cdot\|_\infty) \leq \left(\frac{8C_\rho B_0 e}{\sqrt{2}\epsilon}\right)^{d(W,L)} \leq \left(\frac{16C_\rho B_0}{\epsilon}\right)^{d(W,L)}.$$

Let

$$\varsigma = \left(\frac{16C_\rho B_0}{\epsilon}\right)^{d(W,L)} \exp(-n\epsilon/C^*). \quad (\text{A.16})$$

By the above results and Theorem 1, we have

$$P\left(\mathcal{E}(\hat{f}) - \mathcal{E}(f^*) > (3/2)\epsilon\right) \leq \varsigma. \quad (\text{A.17})$$

Moreover, (A.16) leads to  $\exp(n\epsilon/C^*)\epsilon^{d(W,L)} = (16C_\rho B_0 \varsigma^{-1/d(W,L)})^{d(W,L)}$  which is equivalent to

$$\exp(\varkappa\epsilon)\epsilon = \nu \iff \exp(\varkappa\epsilon)(\varkappa\epsilon) = \varkappa\nu,$$

where  $\varkappa = n/(C^*d(W, L))$  and  $\nu = 16C_\rho B_0 \varsigma^{-1/d(W,L)}$ . Applying the monotone increasing Lambert W-function:  $W : [0, \infty) \rightarrow [0, \infty)$  defined by  $W(t \exp(t)) = t$  on both sides of the above equation, we have

$$W(\varkappa\nu) = \varkappa\epsilon,$$

which is equivalent to  $\epsilon = W(\varkappa\nu)/\varkappa \leq \max(1, \log(\varkappa\nu))/\varkappa$ , since  $W(s) \leq \log(s)$  for all  $s \geq e$ . Then,

$$\begin{aligned} \epsilon &\leq \max(1, \log(\varkappa\nu))/\varkappa = \frac{C^*d(W, L)}{n} \max\left(1, \log \frac{16C_\rho B_0 n}{C^*d(W, L)\varsigma^{1/d(W,L)}}\right) \\ &\leq \frac{C^*d(W, L)}{n} \max\left(1, \log \frac{16C_\rho B_0 n}{C^*d(W, L)\varsigma}\right). \end{aligned}$$

Therefore, we have

$$P\left(\mathcal{E}(\hat{f}) - \mathcal{E}(f^*) > (3/2)\frac{C^*d(W, L)}{n}\max(1, \log\frac{C^{**}n}{d(W, L)\varsigma}\right) \leq \varsigma,$$

for  $C^{**} = 16C_\rho B_0 C^{*-1}$  based on (A.17). Moreover, the result (A.15) implies that

$$C^*d(W, L)\max(1, \log\frac{C^{**}n}{d(W, L)\varsigma}) \leq C^*CWL\log(W)\max(1, \log\frac{C^{**}n}{cWL\log(W/L)\varsigma}).$$

By (A.15) and (A.16), one has  $(\frac{16C_\rho B_0}{\epsilon})^{cWL\log(W/L)}\exp(\frac{-n\epsilon}{C^*}) \leq \varsigma \leq (\frac{16C_\rho B_0}{\epsilon})^{CWL\log(W)}\exp(\frac{-n\epsilon}{C^*})$ . Thus, one has

$$P\left(\mathcal{E}(\hat{f}) - \mathcal{E}(f^*) > \frac{3C^*CWL\log(W)}{2n}\max(1, \log\frac{C^{**}n}{cWL\log(W/L)\varsigma}\right) \leq \varsigma.$$

The proof is complete. □

### A.7 Proofs of Theorem 3

Let  $2^m \asymp n^{1/5}$  and  $m \leq R \asymp \log_2 n$ . When  $d \lesssim (\log_2 n)^{1-\kappa}$  for an arbitrary small constant  $\kappa > 0$ , then for any constant  $c \in (0, \infty)$ ,  $(c(m+d))^{2d} \ll n^\nu$  and  $(c(m+3))^{2d} \ll n^\nu$  for an arbitrary small  $\nu > 0$ . Therefore, the bias term satisfies

$$\begin{aligned}\mathcal{E}(f^*) - \mathcal{E}(f_0) &\leq \zeta_{m,d} \lesssim n^{-4/5}\{(2/3)(m+3)\}^{-2}\{(2/3)(m+3)\}^{2d} \\ &\ll n^{-4/5}(\log_2 n)^{-2}n^\nu = n^{-4/5+\nu}(\log_2 n)^{-2},\end{aligned}$$

where  $\zeta_{m,d}$  is given in (12). Then the bias term satisfies

$$\mathcal{E}(f^*) - \mathcal{E}(f_0) = o(n^{-4/5+\nu}(\log_2 n)^{-2}). \quad (\text{A.18})$$

Moreover, Proposition A.2 leads to

$$\begin{aligned} |V_m^{(1)}| &\lesssim n^{1/5} d^{1/2} \left( \frac{2e}{d-1} \right)^{d-1} (m+d)^{-1} (2e(m+d))^d \\ &\ll n^{1/5} (\log_2 n)^{1/2-\kappa/2} (\log_2 n)^{-1} n^{\nu/2} = n^{1/5+\nu/2} (\log_2 n)^{-\kappa/2-1/2}, \end{aligned}$$

and  $n^{1/5} \lesssim |V_m^{(1)}|$ . Let  $\epsilon = n^{-4/5+\nu/2} (\log_2 n)^{7/2-\kappa/2}$ . By (A.15), one has

$$\begin{aligned} d(W, L) &\asymp (|V_m^{(1)}| + R) L \log(|V_m^{(1)}| + R) \\ &\ll n^{1/5+\nu/2} (\log_2 n)^{-\kappa/2-1/2} (\log_2 n)^2 \log_2(\log_2 n) \\ &= n^{1/5+\nu/2} (\log_2 n)^{3/2-\kappa/2} \log_2(\log_2 n). \end{aligned}$$

Then  $\varsigma$  given in (A.16) satisfies

$$\begin{aligned} \varsigma &\ll \{n^{4/5-\nu/2} (\log_2 n)^{\frac{\kappa-7}{2}}\} n^{1/5+\nu/2} (\log_2 n)^{\frac{3-\kappa}{2}} \log_2(\log_2 n) \exp\{-n^{1/5+\nu/2} (\log_2 n)^{\frac{7-\kappa}{2}}\} \\ &\leq \exp\{n^{1/5+\nu/2} (\log_2 n)^{\frac{3-\kappa}{2}} (\log_2 n) \log_2(\log_2 n)\} \exp\{-n^{1/5+\nu/2} (\log_2 n)^{\frac{7-\kappa}{2}}\} \\ &= \exp\{n^{1/5+\nu/2} (\log_2 n)^{\frac{5-\kappa}{2}} (\log_2(\log_2 n) - \log_2 n)\} \\ &\leq \exp\{-\frac{1}{2} n^{1/5+\nu/2} (\log_2 n)^{\frac{5-\kappa}{2}}\} \end{aligned}$$

, when  $n$  is large. Thus,  $\varsigma \rightarrow 0$  as  $n \rightarrow \infty$ . Therefore, the above results and (A.17) lead to

$$\mathcal{E}(\hat{f}) - \mathcal{E}(f^*) = \mathcal{O}_p(n^{-4/5+\nu/2} (\log_2 n)^{7/2-\kappa/2}). \quad (\text{A.19})$$

The tuning parameter  $\lambda = \mathcal{O}(\epsilon) = \mathcal{O}(n^{-4/5+\nu/2} (\log_2 n)^{7/2-\kappa/2})$ , and  $\varpi_n$  need to satisfy  $\varpi_n = \mathcal{O}(\epsilon) = \mathcal{O}(n^{-4/5+\nu/2} (\log_2 n)^{7/2-\kappa/2})$ .



From the results in (A.18) and (A.19), we have

$$\begin{aligned}
\mathcal{E}(\widehat{f}) - \mathcal{E}(f_0) &= \mathcal{E}(\widehat{f}) - \mathcal{E}(f^*) + \mathcal{E}(f^*) - \mathcal{E}(f_0) \\
&= \mathcal{O}_p(n^{-4/5+\nu/2}(\log_2 n)^{7/2-\kappa/2}) + o(n^{-4/5+\nu}(\log_2 n)^{-2}) \\
&= o_p(n^{-4/5+\nu}(\log_2 n)^{-2}).
\end{aligned}$$

When  $R \asymp \log_2 n$ , the ReLU network that is used to construct the estimator  $\widehat{f}$  has depth  $\mathcal{O}(R \log_2 d) = \mathcal{O}[\log_2 n \{\log_2(\log_2 n)\}]$ , the number of computational units  $\mathcal{O}(Rd) \times |V_m^{(1)}| = \mathcal{O}\{(\log_2 n)^{3/2(1-\kappa)} n^{1/5+\nu/2}\}$ , and the number of weights  $\mathcal{O}(Rd) \times |V_m^{(1)}| = \mathcal{O}\{(\log_2 n)^{3/2(1-\kappa)} n^{1/5+\nu/2}\}$ .

### A.8 Proofs of Proposition 3

Let  $2^m \asymp n^{1/5}$  and  $m \leq R \asymp \log_2 n$ . When  $d$  is a fixed constant not depending on  $n$ , the bias term satisfies

$$\mathcal{E}(f^*) - \mathcal{E}(f_0) \leq \zeta_{m,d} \lesssim n^{-4/5} \{(2/3)(m+3)\}^{2(d-1)} \lesssim n^{-4/5} (\log_2 n)^{2d-2},$$

where  $\zeta_{m,d}$  is given in (12). Then,

$$\mathcal{E}(f^*) - \mathcal{E}(f_0) = \mathcal{O}(n^{-4/5} (\log_2 n)^{2d-2}). \quad (\text{A.20})$$

Moreover, Proposition A.2 leads to

$$|V_m^{(1)}| \lesssim n^{1/5} d^{1/2} (m+d)^{-1} (2e(m+d))^d = \mathcal{O}(n^{1/5} (\log_2 n)^{d-1}),$$

and  $n^{1/5} \lesssim |V_m^{(1)}|$ . Let  $\epsilon = n^{-4/5}(\log_2 n)^{d+3}$ . By (A.15), one has  $d(W, L) \asymp (|V_m^{(1)}| + R)L \log(|V_m^{(1)}| + R) = \mathcal{O}(n^{1/5}(\log_2 n)^{d+1})$ . Then  $\varsigma$  given in (A.16) satisfies

$$\begin{aligned} \varsigma &\lesssim \{n^{4/5}(\log_2 n)^{-d-3}\}^{n^{1/5}(\log_2 n)^{d+1}} \exp\{-n^{1/5}(\log_2 n)^{d+3}\} \\ &\lesssim \exp\{n^{1/5}(\log_2 n)^{d+2}\} \exp\{-n^{1/5}(\log_2 n)^{d+3}\} \\ &= \exp\{n^{1/5}(\log_2 n)^{d+2}(1 - \log_2 n)\} \lesssim \exp\{-\frac{1}{2}n^{1/5}(\log_2 n)^{d+2}\}. \end{aligned}$$

Thus,  $\varsigma \rightarrow 0$  as  $n \rightarrow \infty$ . Therefore, the above results and (A.17) lead to

$$\mathcal{E}(\widehat{f}) - \mathcal{E}(f^*) = \mathcal{O}_p(n^{-4/5}(\log_2 n)^{d+3}). \quad (\text{A.21})$$

The tuning parameter and  $\varpi_n$  need to satisfy  $\varpi_n = \mathcal{O}(\epsilon) = \mathcal{O}(n^{-4/5}(\log_2 n)^{d+3})$  and  $\lambda = \mathcal{O}(\epsilon) = \mathcal{O}(n^{-4/5}(\log_2 n)^{d+3})$ .

From the results in (A.20) and (A.21), we have

$$\begin{aligned} \mathcal{E}(\widehat{f}) - \mathcal{E}(f_0) &= \mathcal{E}(\widehat{f}) - \mathcal{E}(f^*) + \mathcal{E}(f^*) - \mathcal{E}(f_0) \\ &= \mathcal{O}_p(n^{-4/5}(\log_2 n)^{d+3}) + \mathcal{O}(n^{-4/5}(\log_2 n)^{2d-2}) \\ &= \mathcal{O}_p(n^{-4/5}(\log_2 n)^{(d+3) \vee (2d-2)}). \end{aligned}$$

When  $R \asymp \log_2(n)$ , the ReLU network that is used to construct the estimator  $\widehat{f}$  has depth  $\mathcal{O}(R \log_2 d) = \mathcal{O}(\log_2 n)$ , the number of computational units

$$\mathcal{O}(Rd) \times |V_m^{(1)}| = \mathcal{O}\{(\log_2 n) n^{1/5}(\log_2 n)^{d-1}\} = \mathcal{O}\{(\log_2 n)^d n^{1/5}\},$$

and the number of weights  $\mathcal{O}(Rd) \times |V_m^{(1)}| = \mathcal{O}\{(\log_2 n)^d n^{1/5}\}$ .

#### A.9 Proofs of Proposition 4

Let  $d^*(W, L)$  denote the VC-dimension of SDRN, where  $W$  is the number of parameters and  $L$  is the number of layers of SDRN. By the construction of SDRN in Section 4.1,

one has for  $n$  sufficiently large,  $W \asymp |V_m^{(1)}| + R$  and  $L \asymp R \log_2 d$ . By Proposition A.2 and  $2^m \asymp n^{1/5}$ , one has  $n^{1/5} \lesssim |V_m^{(1)}|$ . Moreover, since  $R \asymp \log_2 n$ , one has

$$L \asymp \log_2 n \log_2 d \text{ and } n^{1/5} \lesssim W. \quad (\text{A.22})$$

By equation (2) in (Bartlett et al., 2019), one has  $d^*(W, L) \geq c^* \cdot WL \log(W/L)$ , for some constant  $c^* > 0$ . Moreover, (A.22) implies that there exists a constant  $c^{**} > 0$  such that  $\log(W/L) \geq c^{**} \log_2 n$ . Therefore, by the above results, one has that there exists a constant  $c_0 > 0$  such that for  $n$  sufficiently large,

$$d^*(W, L) - 1 \geq c_0 n^{1/5} (\log_2 n)^2 \log_2 d. \quad (\text{A.23})$$

Furthermore, since  $\mathcal{E}(f^*) - \mathcal{E}(f_0) \geq 0$ , one has

$$\mathcal{E}(\hat{f}) - \mathcal{E}(f_0) = \mathcal{E}(\hat{f}) - \mathcal{E}(f^*) + \mathcal{E}(f^*) - \mathcal{E}(f_0) \geq \mathcal{E}(\hat{f}) - \mathcal{E}(f^*). \quad (\text{A.24})$$

By Theorem 3.6 of (Mohri, Rostamizadeh, & Talwalkar, 2018), one has

$$P \left( \mathcal{E}(\hat{f}) - \mathcal{E}(f^*) > \frac{d^*(W, L) - 1}{32n} \right) \geq 1/100.$$

The above result together with (A.23) and (A.24) implies that

$$P \left( \mathcal{E}(\hat{f}) - \mathcal{E}(f_0) > \frac{c_0 n^{1/5} (\log_2 n)^2 \log_2 d}{32n} \right) \geq 1/100.$$

Let  $c_1 = c_0/32$ . Then, one has

$$P \left( \mathcal{E}(\hat{f}) - \mathcal{E}(f_0) > c_1 n^{-4/5} (\log_2 n)^2 \log_2 d \right) \geq 1/100.$$

### A.10 Proofs of Lemmas 1-3

A lemma is presented below and it is used to prove the lemmas given in Section 6.

**Lemma A.3.** *For any  $f \in \mathcal{F}(R, m, B_0, B_1)$ , one has*

$$\lim_{\delta \rightarrow 0^+} \frac{\mathcal{E}(f^* + \delta(f - f^*)) - \mathcal{E}(f^*)}{\delta} \geq 0.$$

*Proof.* Let  $\delta \in (0, 1)$ . Based on the definition of  $\mathcal{F}(R, m, B_0, B_1)$  given in (7), we can see that  $f_0 + \delta(f - f_0) \in \mathcal{F}(R, m, B_0, B_1)$ . Moreover  $\mathcal{E}(f^* + \delta(f - f^*)) - \mathcal{E}(f^*) \geq 0$  by the definition of  $f^*$  given in (9).  $\square$

*Proof of Lemma 1.* Denote  $t_0 = f^*(\mathbf{x})$  and  $t = f(\mathbf{x})$ . By Taylor's expansion and Assumption 6, we have

$$\rho(t, y) - \rho(t_0, y) = \rho'(t_0, y)(t - t_0) + \int_0^1 2^{-1} \rho''(t_0 + (t - t_0)\omega, y)(t - t_0)^2 d\omega.$$

Moreover, by the dominated convergence theorem and Lemma A.3,

$$\begin{aligned} & \int_{\mathcal{X} \times \mathcal{Y}} \rho'(f^*(\mathbf{x}), y)(f(\mathbf{x}) - f^*(\mathbf{x})) d\mu(\mathbf{x}, y) \\ &= \int_{\mathcal{X} \times \mathcal{Y}} \lim_{\delta \rightarrow 0^+} \frac{\rho(f^* + \delta(f - f^*), y) - \rho(f^*, y)}{\delta} d\mu(\mathbf{x}, y) \\ &= \lim_{\delta \rightarrow 0^+} \int_{\mathcal{X} \times \mathcal{Y}} \frac{\rho(f^* + \delta(f - f^*), y) - \rho(f^*, y)}{\delta} d\mu(\mathbf{x}, y) \\ &= \lim_{\delta \rightarrow 0^+} \frac{\mathcal{E}(f^* + \delta(f - f^*)) - \mathcal{E}(f^*)}{\delta} \geq 0. \end{aligned}$$

Therefore,

$$\begin{aligned} \mathcal{E}(f) - \mathcal{E}(f^*) &= \int_{\mathcal{X} \times \mathcal{Y}} \{\rho(f(\mathbf{x}), y) - \rho(f^*(\mathbf{x}), y)\} d\mu(\mathbf{x}, y) \\ &\geq \int_{\mathcal{X} \times \mathcal{Y}} a_\rho (f(\mathbf{x}) - f^*(\mathbf{x}))^2 d\mu(\mathbf{x}, y) = a_\rho \|f - f^*\|_2^2. \end{aligned}$$

Since  $\int_{\mathcal{Y}} \rho'(f_0(\mathbf{x}), y) d\mu(y|\mathbf{x}) = 0$ , then  $\int_{\mathcal{X} \times \mathcal{Y}} \rho'(f_0(\mathbf{x}), y)(f(\mathbf{x}) - f_0(\mathbf{x})) d\mu(\mathbf{x}, y)$

= 0. Thus,

$$\begin{aligned}\mathcal{E}(f) - \mathcal{E}(f_0) &= \int_{\mathcal{X} \times \mathcal{Y}} (\rho(f(\mathbf{x}), y) - \rho(f_0(\mathbf{x}), y)) d\mu(\mathbf{x}, y) \\ &\leq \int_{\mathcal{X} \times \mathcal{Y}} b_\rho (f(\mathbf{x}) - f_0(\mathbf{x}))^2 d\mu(\mathbf{x}, y) = b_\rho \|f - f_0\|_2^2.\end{aligned}$$

□

*Proof of Lemma 2.* In the following, we will show the results in Lemma 2 when the loss function  $\rho(f(\mathbf{x}), y)$  is the quantile loss given in (3). We follow a proof procedure from (Alquier et al., 2019). We have

$$\begin{aligned}\mathcal{E}(f) - \mathcal{E}(f^*) &= \int_{\mathcal{X} \times \mathcal{Y}} (\rho(f(\mathbf{x}), y) - \rho(f^*(\mathbf{x}), y)) d\mu(\mathbf{x}, y) \\ &= \int_{\mathcal{X}} \int_{\mathcal{Y}} (\rho(f(\mathbf{x}), y) - \rho(f^*(\mathbf{x}), y)) d\mu(y|\mathbf{x}) d\mu_X(\mathbf{x})\end{aligned}$$

Then for all  $\mathbf{x} \in \mathcal{X}$ ,

$$\begin{aligned}&\int_{\mathcal{Y}} \rho(f(\mathbf{x}), y) d\mu(y|\mathbf{x}) \\ &= \int_{\mathcal{Y}} I\{y > f(\mathbf{x})\} (y - f(\mathbf{x})) d\mu(y|\mathbf{x}) + (\tau - 1) \int_{\mathcal{Y}} (y - f(\mathbf{x})) d\mu(y|\mathbf{x}) \\ &= g(\mathbf{x}, f(\mathbf{x})) + (\tau - 1) \int_{\mathcal{Y}} y d\mu(y|\mathbf{x}),\end{aligned}$$

where  $g(\mathbf{x}, u) = \int_{\mathcal{Y}} I\{y > u\} (1 - \mu(y|\mathbf{x})) dy + (1 - \tau)u$ , and  $\mathcal{E}(f) - \mathcal{E}(f^*) = \int_{\mathcal{X}} g(\mathbf{x}, f(\mathbf{x})) d\mu_X(\mathbf{x}) - \int_{\mathcal{X}} g(\mathbf{x}, f^*(\mathbf{x})) d\mu_X(\mathbf{x})$ . Denote  $t_0 = f^*(\mathbf{x})$  and  $t = f(\mathbf{x})$ .

By Taylor's expansion, we have

$$g(\mathbf{x}, t) - g(\mathbf{x}, t_0) = g'(\mathbf{x}, t_0)(t - t_0) + \int_0^1 2^{-1} g''(\mathbf{x}, t_0 + (t - t_0)\omega) (t - t_0)^2 d\omega.$$

Since  $(g(\mathbf{x}, f^* + \delta(f - f^*)) - g(\mathbf{x}, f^*(\mathbf{x}))) / \delta \leq (2 - \tau)|f(\mathbf{x}) - f^*(\mathbf{x})|$ , by the

dominated convergence theorem and Lemma A.3,

$$\begin{aligned}
& \int_{\mathcal{X}} g'(\mathbf{x}, f^*(\mathbf{x}))(f(\mathbf{x}) - f^*(\mathbf{x}))d\mu_X(\mathbf{x}) \\
&= \int_{\mathcal{X}} \lim_{\delta \rightarrow 0^+} \frac{g(\mathbf{x}, f^* + \delta(f - f^*)) - g(\mathbf{x}, f^*(\mathbf{x}))}{\delta} d\mu_X(\mathbf{x}) \\
&= \lim_{\delta \rightarrow 0^+} \int_{\mathcal{X} \times \mathcal{Y}} \frac{g(\mathbf{x}, f^* + \delta(f - f^*)) - g(\mathbf{x}, f^*(\mathbf{x}))}{\delta} d\mu_X(\mathbf{x}) \\
&= \lim_{\delta \rightarrow 0^+} \frac{\mathcal{E}(f^* + \delta(f - f^*)) - \mathcal{E}(f^*)}{\delta} \geq 0.
\end{aligned}$$

The above results together with  $\partial^2 g(\mathbf{x}, u)/\partial u^2 = \mu'(u|\mathbf{x})$  imply that

$$\begin{aligned}
& \mathcal{E}(f) - \mathcal{E}(f^*) \\
&= \int_{\mathcal{X}} \{g(\mathbf{x}, f(\mathbf{x})) - g(\mathbf{x}, f^*(\mathbf{x}))\} d\mu_X(\mathbf{x}) \\
&\geq 2^{-1} \int_{\mathcal{X}} (f(\mathbf{x}) - f^*(\mathbf{x}))^2 \int_0^1 g''(\mathbf{x}, f^*(\mathbf{x}) + (f(\mathbf{x}) - f^*(\mathbf{x}))\omega) d\omega d\mu_X(\mathbf{x}) \\
&= 2^{-1} \int_{\mathcal{X}} (f(\mathbf{x}) - f^*(\mathbf{x}))^2 \int_0^1 \mu'(f^*(\mathbf{x}) + (f(\mathbf{x}) - f^*(\mathbf{x}))\omega|\mathbf{x}) d\omega d\mu_X(\mathbf{x}) \\
&\geq \frac{1}{2C_1} \int_{\mathcal{X}} (f(\mathbf{x}) - f^*(\mathbf{x}))^2 d\mu_X(\mathbf{x}) = \frac{1}{2C_1} \|f - f^*\|_2^2.
\end{aligned}$$

Note that  $\partial g(\mathbf{x}, u)/\partial u|_{u=f_0} = 0$  and  $\partial^2 g(\mathbf{x}, u)/\partial u^2 = \mu'(u|\mathbf{x})$ . Thus by Taylor's expansion,

$$\begin{aligned}
& \mathcal{E}(f) - \mathcal{E}(f_0) \\
&= \int_{\mathcal{X}} \{g(\mathbf{x}, f(\mathbf{x})) - g(\mathbf{x}, f_0(\mathbf{x}))\} d\mu_X(\mathbf{x}) \\
&= 2^{-1} \int_{\mathcal{X}} (f(\mathbf{x}) - f_0(\mathbf{x}))^2 \int_0^1 g''(\mathbf{x}, f_0(\mathbf{x}) + (f(\mathbf{x}) - f_0(\mathbf{x}))\omega) d\omega d\mu_X(\mathbf{x}) \\
&= 2^{-1} \int_{\mathcal{X}} (f(\mathbf{x}) - f_0(\mathbf{x}))^2 \int_0^1 \mu'(f_0(\mathbf{x}) + (f(\mathbf{x}) - f_0(\mathbf{x}))\omega|\mathbf{x}) d\omega d\mu_X(\mathbf{x}) \\
&\leq \frac{1}{2C_2} \int_{\mathcal{X}} (f(\mathbf{x}) - f_0(\mathbf{x}))^2 d\mu_X(\mathbf{x}) = \frac{1}{2C_2} \|f - f_0\|_2^2.
\end{aligned}$$

□

*Proof of Lemma 3.* The proof of Lemma 3 follows the same procedure as the proof of Lemma 2, and thus it is omitted.  $\square$

## References

- Alquier, P., Cottet, V., & Lecué, G. (2019). Estimation bounds and sharp oracle inequalities of regularized procedures with lipschitz loss functions. *The Annals of Statistics*, 47, 2117–2144.
- Anthony, M., & Bartlett, P. L. (2009). *Neural network learning: Theoretical foundations*. Cambridge University Press.
- Bartlett, P. L., Harvey, N., Liaw, C., & Mehrabian, A. (2019). Nearly-tight vc-dimension and pseudodimension bounds for piecewise linear neural networks. *Journal of Machine Learning Research*, 63, 1–17.
- Bauer, B., & Kohler, M. (2019). On deep learning as a remedy for the curse of dimensionality in nonparametric regression. *The Annals of Statistics*, 47, 2261–2285.
- Bellman, R. (1961). *Curse of dimensionality. adaptive control processes: a guided tour*. Princeton, NJ.
- Bengio, Y., & LeCun, Y. (2007). *Scaling learning algorithms towards ai. in bottou, l., chapelle, o., and decoste, d. and weston, j., eds., Large-Scale Kernel Machines*. MIT Press.
- Bungartz, H. J., & Griebel, M. (2004). Sparse grids. *Acta Numerica*.
- Chen, M., Jiang, H., Liao, W., & Zhao, T. (2022). Nonparametric regression on low-dimensional manifolds using deep relu networks. *Information and Inference: A Journal of the IMA*, 11, 1203–1253.
- Chen, Y., Segovia-Dominguez, I., & Gel, Y. R. (2021). Z-gcnets: Time zigzags at graph convolutional networks for time series forecasting. *International Conference on Machine Learning (ICML)*, 1684-1694.
- Cheng, M. Y., Fan, J., & Marron, J. S. (1994). Minimax efficiency of local polynomial fit estimators at boundaries. *Mimeo Series 2098, University of North Carolina*

*Chapel Hill.*

- Cheng, M. Y., & Wu, H. T. (2013). Local linear regression on manifolds and its geometric interpretation. *Journal of the American Statistical Association*, *108*, 1421–1434.
- Cucker, F., & Zhou, D. (2007). *Learning theory*. Cambridge Monographs on Applied and Computational Mathematics.
- Dua, D., & Graff, C. (2019). Uci machine learning repository [<http://archive.ics.uci.edu/ml>]. Irvine, CA: University of California, School of Information and Computer Science.
- Eldan, R., & Shamir, O. (2016). The power of depth for feedforward neural networks. *JMLR: Workshop and Conference Proceedings*, 1-34.
- Fan, J., & Gijbels, I. (1996). *Local polynomials modelling and its applications*. Chapman and Hall, London.
- Fan, J., & Huang, T. (2005). Profile likelihood inferences on semiparametric varying-coefficient partially linear models. *Bernoulli*, *11*, 1031–1057.
- Fan, J., Ma, C., & Zhong, Y. (2021). A selective overview of deep learning. *Statistical Science*, *36*, 264-290.
- Griebel, M. (2006). Sparse grids and related approximation schemes for higher dimensional problems. *Foundations of Computational Mathematics, Cambridge University Press*, 106-161.
- Harrison Jr, D., & Rubinfeld, D. L. (1978). Hedonic housing prices and the demand for clean air. *Journal of Environmental Economics and Management*, *5*, 81–102.
- Kingma, D. P., & Ba, J. L. (2015). Adam: a method for stochastic optimization. *International Conference on Learning Representations*.
- Kohler, M., & Mehnert, J. (2011). Analysis of the rate of convergence of least squares neural network regression estimates in case of measurement errors. *Neural Networks*, *24*, 273–279.
- Kotsiantis, S. (2007). Supervised machine learning: A review of classification tech-



- niques. *Informatica*, 31, 249-268.
- Kůrková, V., & Sanguineti, M. (2019). Classification by sparse neural networks. *IEEE Transactions on Neural Networks and Learning Systems*, 30, 2746-2754.
- LeCun, Y., Bengio, Y., & Hinton, G. (2015). Deep learning. *Nature*, 521, 436–444.
- Li, B., Tang, S., & Yu, H. (2020). Better approximations of high dimensional smooth functions by deep neural networks with rectified power units. *Communications in Computational Physics*, 27, 379–411.
- Liang, S., & Srikant, R. (2017). Why deep neural networks for function approximation? *International Conference on Learning Representations*.
- Lin, S.-B., Wang, K., Wang, Y., & Zhou, D.-X. (2022). Universal consistency of deep convolutional neural networks. *IEEE Transactions on Information Theory*, 68, 4610-4617.
- Ma, S., Racine, J., & Yang, L. (2015). Spline regression in the presence of categorical predictors. *Journal of Applied Econometrics*, 30, 705–717.
- Mao, T., & Zhou, D.-X. (2022a). Approximation of functions from korobov spaces by deep convolutional neural networks. *Advances in Computational Mathematics*, 1, 48–84.
- Mao, T., & Zhou, D.-X. (2022b). Approximation of functions from korobov spaces by deep convolutional neural networks. *Advances in Computational Mathematics*, 48(6), 84.
- McDermott, J., & Forsyth, R. S. (2016). Diagnosing a disorder in a classification benchmark. *Pattern Recognition Letters*, 73, 41–43.
- Mhaskar, H., Liao, Q., & Poggio, T. (2017). When and why are deep networks better than shallow ones? *Proceedings of the Thirty-First AAAI Conference on Artificial Intelligence*, 2343-2349.
- Mhaskar, H., & Poggio, T. (2016). Deep vs. shallow networks: An approximation theory perspective. *Analysis and Applications*, 14, 829-848.
- Mohri, M., Rostamizadeh, A., & Talwalkar, A. (2018). *Foundations of machine learn-*

- ing. MIT Press.
- Montanelli, H., & Du, Q. (2019). New error bounds for deep relu networks using sparse grids. *SIAM Journal on Mathematics of Data Science*, *1*, 78–92.
- Nakada, R., & Imaizumi, M. (2020). Adaptive approximation and generalization of deep neural network with intrinsic dimensionality. *Journal of Machine Learning Research*, *21*, 1–38.
- Poggio, T., Mhaskar, H. N., Rosasco, L., Miranda, B., & Liao, Q. (2017). Why and when can deep-but not shallow-networks avoid the curse of dimensionality: A review. *International Journal of Automation and Computing*, *14*, 503–519.
- Ruppert, D. (1997). Empirical-bias bandwidths for local polynomial nonparametric regression and density estimation. *Journal of the American Statistical Association*, *92*, 1049-1062.
- Schmidhuber, J. (2015). Deep learning in neural networks: An overview. *Neural Networks*, *61*, 85–117.
- Schmidt-Hieber, J. (2019). Deep relu network approximation of functions on a manifold. *preprint*, <https://arxiv.org/abs/1908.00695>.
- Schmidt-Hieber, J. (2020). Nonparametric regression using deep neural networks with relu activation function. *The Annals of Statistics*, *48*, 1875–1897.
- Shaham, U., Cloninger, A., & Coifman, R. R. (2018). Provable approximation properties for deep neural networks. *Applied and Computational Harmonic Analysis*, *44*(3), 537–557.
- Shen, J., & Wang, L. L. (2010). Sparse spectral approximations of high-dimensional problems based on hyperbolic cross. *SIAM Journal on Numerical Analysis*, *48*, 1087-1109.
- Shen, Z., Yang, H., & Zhang, S. (2020). Deep network approximation characterized by number of neurons. *Communications in Computational Physics*, *28*, 1768–1811.
- Srivastava, N., Hinton, G., Krizhevsky, A., Sutskever, I., & Salakhutdinov, R. (2014). Dropout: A simple way to prevent neural networks from overfitting. *Journal of*

- Machine Learning Research*, 15, 1929-1958.
- Stone, C. J. (1982). Optimal global rates of convergence for nonparametric regression. *The Annals of Statistics*, 10, 1040–1053.
- Stone, C. J. (1985). Additive regression and other nonparametric models. *The Annals of Statistics*, 13, 689–705.
- Stone, C. J. (1994). The use of polynomial splines and their tensor products in multivariate function estimation. *The Annals of Statistics*, 22, 118–184.
- Stone, C. J., Hansen, M. H., Kooperberg, C., & Truong, Y. K. (1997). Polynomial splines and their tensor products in extended linear modeling: 1994 wald memorial lecture. *The Annals of Statistics*, 25, 1371–1470.
- Wang, D., & Chen, J. (2018). Supervised speech separation based on deep learning: An overview. *IEEE/ACM Transactions on Audio, Speech, and Language Processing*, 26, 1702-1726.
- Wasserman, L. (2006). *All of nonparametric statistics*. Springer Texts in Statistics.
- Yarotsky, D. (2017). Error bounds for approximations with deep relu networks. *Neural Networks*, 70, 103–114.